JOC Article

Fine Tuning of Electrostatics around the Internucleotidic Phosphate through Incorporation of Modified 2′,4′-Carbocyclic-LNAs and -ENAs Leads to Significant Modulation of Antisense Properties

Chuanzheng Zhou, Yi Liu, Mounir Andaloussi, Naresh Badgujar, Oleksandr Plashkevych, and Jyoti Chattopadhyaya*

Department of Bioorganic Chemistry, Box 581, Biomedical Center, Uppsala University, SE-751 23 Uppsala, Sweden

jyoti@boc.uu.se

Received July 28, 2008

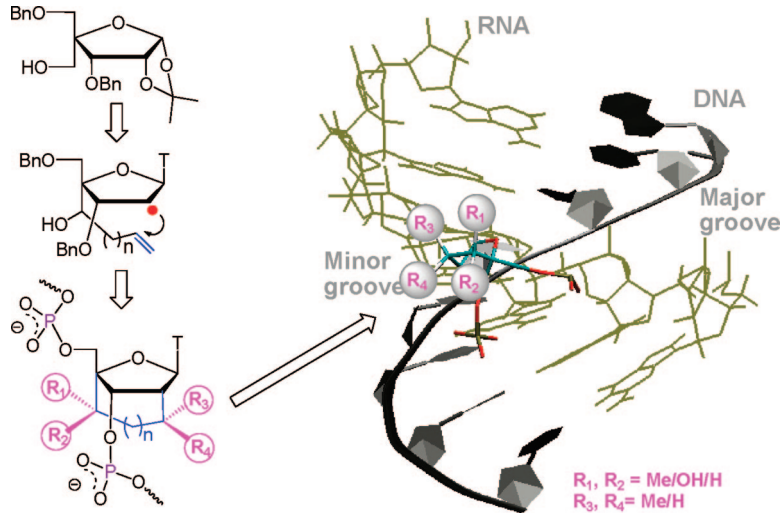

In the antisense (AS) and RNA interference (RNAi) technologies, the native single-stranded 2′-deoxyoligonucleotides (for AS) or double-stranded RNA (for RNAi) are chemically modified to bind to the target RNA in order to give improved downregulation of gene expression through inhibition of RNA translation. It is shown here how the fine adjustment of the electrostatic interaction by alteration of the substituents as well as their stereochemical environment around the internucleotidic phosphodiester moiety near the edge of the minor grove of the antisense oligonucleotides (AON)-RNA heteroduplex can lead to the modulation of the antisense properties. This was demonstrated through the synthesis of various modified carbocyclic-locked nucleic acids (LNAs) and -ethylene-bridged nucleic acids (ENAs) with hydroxyl and/or methyl substituents attached at the carbocyclic part and their integration into AONs by solid-phase DNA synthesis. The target affinity toward the complementary RNA and DNA, nuclease resistance, and RNase H elicitation by these modified AONs showed that both the nature of the modification (-OH versus -CH_3) and their respective stereochemical orientations vis-à-vis vicinal phosphate play a very important role in modulating the AON properties. Whereas the affinity to the target RNA and the enzymatic stability of AONs were not favored by the hydrophobic and sterically bulky modifications in the center of the minor groove, their positioning at the edge of the minor groove near the phosphate linkage resulted in significantly improved nuclease resisitance without loss of target affinity. On the other hand, hydrophilic modification, such as a hydroxyl group, close to the phosphate linkage made the internucleotidic phosphodiester especially nucleolytically unstable, and hence was not recommended. The substitutions on the carbocyclic moiety of the carba-LNA and -ENA did not affect significantly the choice of the cleavage sites of RNase H mediated RNA cleavage in the AON/RNA hybrid duplex, but the cleavage rate depended on the modification site in the AON sequence. If the original preferred cleavage site by RNase H was included in the 4-5nt stretch from the 3′-end of the modification site in the AON, decreased cleavage rate was observed. Upon screening of 52 modified AONs, containing 13 differently modified derivatives at C6′ and C7′ (or C8′) of the carba-LNAs and -ENAs, two excellent modifications in the carba-LNA series were identified, which synergistically gave outstanding antisense properties such as the target RNA affinity, nuclease resistance, and RNase H activity and were deemed to be ideal candidates as potential antisense or siRNA therapeutic agents.

10.1021/jo8016742 CCC: $40.75
Published on Web 12/04/2008

Introduction

The antisense technology[1,2] and RNA interference (RNAi)[3] are important approaches to downregulate gene expression through inhibition of RNA translation. In these approaches, single-stranded oligonucleotides (for antisense) or double-stranded RNA (for RNAi) are designed to bind to target RNA through Watson−Crick base paring, followed by degradation of target RNA, ideally, through the RNase H (for antisense)[4] pathway or through a RNA-induced silencing complex (RISC, for RNAi) mediated mechanism.[5] Native oligoribonucleotides do not have acceptable pharmacokinetic and pharmacodynamic properties[6,7] mainly because of lack of nuclease resistance. This has stimulated enormous chemical efforts to produce therapeutically significant modified oligonucleotides to provide improved stability, while maintaining high target affinity and specificity and eliciting RNase H activity or RISC recruitment properties in both antisense[8] and siRNA technologies.[7,9]

AONs with direct chemical modification of the phosphodiester linkage to the phosphorothioate have shown improved nuclease resistance[10,11] but reduced affinity towards a complementary RNA sequence.[11] The second generation of AON [12,13] involve various 2′-modifications of the ribose moiety with appropriate electronegative substituents. This modification can confer an RNA-like 3′-*endo* sugar puckering, which results in a considerable improvement of binding affinity to the target RNA.[14] The size, electronegativity, and configuration of the 2′-substituents are all very important factors for the target affinity and nuclease resistance.[15,16] The new third generation of antisense oligonucleotides, containing conformationally constrained LNA[17] (also called BNA[18]) and its 6′-alkylated derivatives[19,20] or ENA[21] modifications,[22,23] have rigid bicyclic ring systems that result in typical locked 3′-*endo* conformation of the sugar puckering.[24] Oligonucleotides containing LNA or ENA are preorganized in the A-type canonical structure,[25] which shows unusually high affinity toward complementary RNA strand (3−8 °C per modification).[21,26] Unfortunately, though LNA and ENA containing AONs are more nucleolytically stable than the native PO AONs, they do not have nuclease resistance as good as that of the PS AONs.[27]

Recently, the synthesis of the conformationally-locked five-membered 2′,4′-carbocyclic-LNA (carba-LNA) and six-membered 2′,4′-carbocyclic-ENA (carba-ENA) thymidine analogs through free-radical cyclization[28] was reported by our group. The homo- and heteroduplexes of these carba-LNA or -ENA substituted AONs showed thermal stabilities comparable to those of their LNA and ENA counterparts. they also showed unprecedented blood serum stability (>48 h) and uncompromised RNase H recruitment capability, which was comparable to those of the native counterparts.[28] We argued that the rigidity of the 2′,4′-carbocycle in the carba-LNA or -ENA molecules, together with the unique antisense properties they confer to their AONs, make them very attractive scaffolds for further functionalization. This in turn might allow us to modulate important properties such as steric clash,[29] hydration pattern,[30−35] or other electrostatic effects[36−38] around phosphodiester linkage in its homo- or heteroduplex form.

It is shown here that it is possible to carefully engineer the chemical (electrostatic) environment around the phosphodiester moiety by modification of the carbocyclic part of the carba-LNA and -ENA with bulky, hydrophobic methyl and/or hydrophilic hydroxyl groups. These specific modifications have subsequently led to successful modulation of both the nuclease resistance and duplex thermal stability without compromising the RNase H activity.

Results and Discussion

1. Synthesis of the Modified Carba-LNA and ENA Thymidine Building Blocks. As shown in the retrosynthetic analysis in Scheme 1, the C6′ site in 7′-methyl carba-LNA or 8′-methyl carba-ENA is closest ($d_{C6'-P} \approx 4$ Å) to the adjacent phosphodiester linkage (compound **1**). This spatial proximity

(1) Zamecnik, P. C.; Stephenson, M. L. *Proc. Natl. Acad. Sci. U.S.A.* **1978**, *75*, 280–284.
(2) Stephenson, M. L.; Zamecnik, P. C. *Proc. Natl. Acad. Sci. U.S.A.* **1978**, *75*, 285–288.
(3) Fire, A.; Xu, S.; Montgomery, M. K.; Kostas, S.; Driver, S. E.; Mello, C. C. *Nature* **1998**, *391*, 806–811.
(4) Kurreck, J. *Eur. J. Biochem.* **2003**, *270*, 1628–1644.
(5) Meister, G.; Tuschl, T. *Nature* **2004**, *431*, 343–349.
(6) Crooke, S. *Annu. Rev. Med.* **2004**, *55*, 61–95.
(7) Bumcrot, D.; Manoharan, M.; Koteliansky, V.; Sah, D. W. Y. *Nat. Chem. Biol.* **2006**, *2*, 711–719.
(8) Uhlmann, E.; Peyman, A. *Chem. Rev.* **1990**, *90*, 543–584.
(9) Manoharan, M. *Curr. Opin. Chem. Biol.* **2004**, *8*, 570–579.
(10) Campbell, J. M.; Bacon, T. A.; Wickstrom, E. *J. Biochem. Biohphys. Methods* **1990**, *20*, 259–267.
(11) Levin, A. A. *Biochim. Biophys. Acta* **1999**, *1489*, 69–84.
(12) Manoharan, M. *Biochim. Biophys. Acta* **1999**, *1489*, 117–130.
(13) Freier, S. M.; Altmann, K. H. *Nucleic Acids Res.* **1997**, *25*, 4429–4443.
(14) Kawasaki, A. W.; Casper, M. D.; Freier, S. M.; Lesnik, E. A.; Zounes, M. C.; Cummins, L. L.; Gonzalez, C.; Cook, P. D. *J. Med. Chem* **1993**, *36*, 831–841.
(15) Cummins, L. L.; Owens, S. S.; Risen, L. M.; Lesnik, E. A.; Freier, S. M.; McGee, D.; Guinosso, C. J.; Cook, P. D. *Nucleic Acids Res.* **1995**, *23*, 2019–2024.
(16) Lesnik, E. A.; Guinosso, C. J.; Kawasaki, A. W.; Sasmor, H.; Zounes, M.; Cummins, L. L.; Ecker, D.; Cook, P. D.; Freier, S. M. *Biochemistry* **1993**, *32*, 7832–7838.
(17) Singh, S. K.; Nielsen, P.; Koshkin, A. A.; Wengel, J. *Chem. Commun.* **1998**, 455–456.
(18) Obika, S.; Morio, K.; Nanbu, D.; Imanishi, T. *Chem. Commun.* **1997**, 1643–1644.
(19) Swayze, E. E.; Seth, P. P. Patent WO2007090071, 2007.
(20) Enderlin, G.; Nielsen, P. *J. Org. Chem.* **2008**, *73*, 6891–6894.
(21) Morita, K.; Hasegawa, C.; Kaneko, M.; Tsutsumi, S.; Sone, J.; Ishikawa, T.; Imanishi, T.; Koizumi, M. *Bioorg. Med. Chem. Lett.* **2002**, *12*, 73–76.
(22) Albak, N.; Petersen, M.; Nielsen, P. *J. Org. Chem.* **2006**, *71*, 7731–7740.
(23) Abdur Rahman, S. M.; Seki, S.; Obika, S.; Yoshikawa, H.; Miyashita, K.; Imanishi, T. *J. Am. Chem. Soc.* **2008**, *130*, 4886–4896.
(24) Obika, S.; Nanbu, D.; Hari, Y.; Morio, K.; In, Y.; Ishida, T.; Imanishi, T. *Tetrahedron Lett.* **1997**, *38*, 8735–8738.
(25) Petersen, M.; Bondensgaard, K.; Wengel, J.; Jacobsen, J. P. *J. Am. Chem. Soc.* **2002**, *124*, 5974–5982.
(26) Koshkin, A. A.; Singh, S. K.; Nielsen, P. R. V. K.; Kumar, R. M. M.; Olsen, C. E.; Wengel, J. *Tetrahedron* **1998**, *54*, 3607–3630.
(27) Morita, K.; Takagi, M.; Hasegawa, C.; Kaneko, M.; Tsutsumi, S.; Sone, J.; Ishikawa, T.; Imanishi, T.; Koizumi, M. *Bioorg. Med. Chem.* **2003**, *11*, 2211–2226.
(28) Srivastava, P.; Barman, J.; Pathmasiri, W.; Plashkevych, O.; Wenska, M.; Chattopadhyaya, J. *J. Am. Chem. Soc.* **2007**, *129*, 8362–8379.
(29) Pattanayek, R.; Sethaphong, L.; Pan, C.; Prhavc, M.; Prakash, T. P.; Manoharan, M.; Egli, M. *J. Am. Chem. Soc.* **2004**, *126*, 15006–15007.
(30) Teplova, M.; Minasov, G.; Tereshko, V.; Inamati, G. B.; Cook, P. D.; Manoharan, M.; Egli, M. *Nat. Struct. Biol.* **1999**, *6*, 535–539.
(31) Egli, M.; Minasov, G.; Teplova, M.; Kumar, R.; Wengel, J. *Chem. Commun.* **2001**, 651–652.
(32) Schneider, B.; Patel, K.; Berman, H. M. *Biophys. J* **1998**, *75*, 2422–2434.
(33) Tereshko, V.; Gryaznov, S.; Egli, M. *J. Am. Chem. Soc.* **1998**, *120*, 269–283.
(34) Auffinger, P.; Westhof, E. *Angew. Chem., Int. Ed.* **2001**, *40*, 4648–4650.
(35) Ball, P. *Chem. Rev.* **2008**, *108*, 74–108.
(36) Griffey, R. H.; Monia, B. P.; Cummins, L. L.; Freier, S. M.; Greig, M. J.; Guinosso, C. J.; Lesnik, E.; Manalili, S. M.; Mohan, V.; Owens, S.; Ross, B. R.; Sasmor, H.; Wancewicz, E.; Weiler, K.; Wheeler, P. D.; Cook, P. D. *J. Med. Chem.* **1996**, *39*, 5100–5109.
(37) Prhavc, M.; Prakash, T. P.; Minasov, G.; Cook, P. D.; Egli, M.; Manoharan, M. *Org. Lett.* **2003**, *5*, 2017–2020.

SCHEME 1

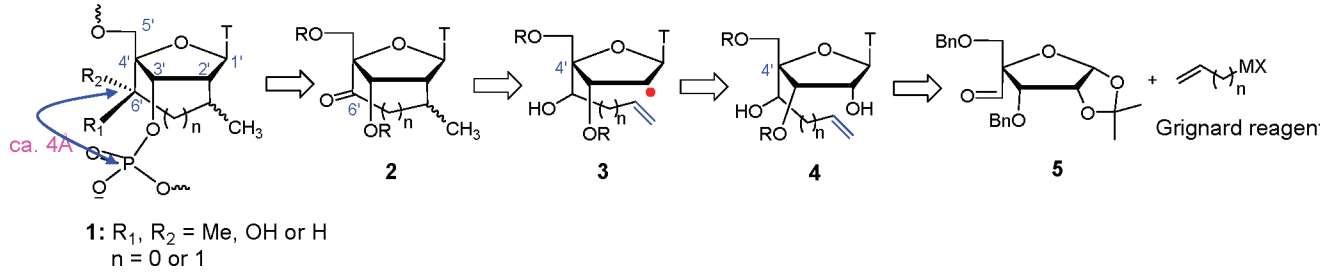

suggests that the hydration pattern around the adjacent phosphate could be modulated by introducing steric and/or polar effect through introduction of a simple substituent such as a hydroxyl and/or methyl group at C6′ (R_1 and R_2 in compound **1** in Scheme 1). This is particularly attractive because 6′-OH and/or 6′-Me can easily be derived from the cyclic ketone **2**. This cyclic ketone, on the other hand, can be obtained by free radical cyclization[28] of the hydroxyl olefin **3**. The key cyclization precursor **3** can be easily synthesized from aldehyde **5**[28,39] with Grignard reagent. In order to shorten our synthetic route and avoid side reactions, we decided to build up the 4′-alkyl side chain through the Grignard reaction before the glycosylation step with thymine.

The synthetic route to the modified carba-LNAs is shown in Scheme 2. The synthesis started from the known precursor **6**,[39] which was oxidized through Swern oxidation to the corresponding aldehyde **5**. The crude aldehyde was subjected to Grignard reaction with vinylmagnesium bromide at room temperature overnight to give the C6′-hydroxyl olefin **7** in high yield (84% in two steps). TLC and NMR showed that the olefin **7** is a pure isomer; no configuration at C6′ could be confirmed by nuclear Overhauser effect (NOE) experiment at this stage. This could however be confirmed only after the free-radical cyclization step (see below), which subsequently showed the C6′-*S* stereochemistry of **7** after the Grignard reaction. Acetylation of **7** using a mixture of acetic anhydride, acetic acid, and triflic acid gave the corresponding triacetate **8** as an anomeric mixture. The crude **8** was subjected to a modified Vorbruggen reaction involving in situ silylation of thymine and subsequent trimethylsilyl triflate-mediated coupling to give exclusively β-D-ribofuranosyl thymine derivative **9**.[39] Deacetylation of **9** using 30% methylamine in ethanol at room temperature overnight gave compound **10** quantitatively, which was esterified with phenyl chlorothioformate to give the key precursor **11** for the free-radical cyclization. The esterification of **10** to **11** was fast, highly selective, and high yielding (92%). The 2′-*O*-phenoxythiocarbonyl (PTC) derivative **11** was found to be the sole product even when 2.5 equiv of phenyl chlorothioformate was used. The key free-radical cyclization was carried out in refluxing anhydrous toluene with the Bu_3SnH, using AIBN as the initiator, which were added dropwise in order to avoid the side reactions. Just as reported before,[28] the 5-hexenyl radical cyclization proceeded in the 5-*exo* cyclization mode to give **12a** (with C7′ methyl at the pseudoequatorial position, 7′*S*) as the major product along with the minor product **12b** (with C7′ methyl being pseudoaxial, 7′*R*). In addition, 1D NOE experiments (Figures SIII.1 and SIII.2) of **12a** and **12b** also showed that they have the C6′*S* stereochemistry, which also proved that the Grignard reaction took place exclusively to give **7** (**6** →**7**) with C6′*S* stereochemistry. The **12a** and **12b** were oxidized to the corresponding ketones **13a** and **13b** with Dess−Martin periodinane, followed by reduction with $NaBH_4$. For **12b**, this oxidization-reduction sequence [**12b** → **13b** (73%) → **14b** (90%)] resulted in complete inversion of configuration at C6′ in **14b**, while the reduction of **13a** gave the two isomers **14a** and **12a** in 6/4 ratio. This differential stereoselectivity for reduction of **13a** and **13b** can be easily understood from the fact that in **13b**, the bulkyl 7′-methyl and 3′-*O*-Bn pointed to the same side of the carbocycle (i.e., above the ring) and hence hydride attacked predominantly from below the plane of the carbocycle ring owing to the steric hindrance at the top. On the other hand, in **13a** the orientation of 3′-*O*-Bn (located above the plain of the carbocycle) and 7′-methyl (located below the plain of the carbocycle) were opposite, and therefore the hydride attack was relatively less selective, suggesting that both the top and the bottom sides of the carba-ring may have similar steric hindrance.

To synthesize the phosphoramidites of **12a**, **12b**, **14a**, and **14b** for solid-support DNA synthesis, the 6′-OH should be protected with an acetyl group. Unfortunately, it was found that 6′-*O*-acetate was unstable during the debenzylation by hydrogenolysis. The 6′-*O*-(*p*-toluoyl) group, however, proved to be a good choice to circumvent this. Thus, compounds **15a** and **15b** could be debenzylated completely using 20% $Pd(OH)_2$/C (500 mg/mmol substrate) and ammonium formate (20 equiv) under reflux in methanol for 4 h, without any toluoyl ester cleavage being detected, followed by 5′-dimethoxytritylation to give **16a** and **16b** in 70% and 63% yields, respectively. However, under the same condition, debenzylation of **15c** gave a byproduct beside the desired product **15c′**. The amount of this byproduct increased with prolongation of the reaction time. NMR analysis of the byproduct showed it was formed by transfer of the 6′-*O*-(*p*-toluoyl) group to the primary 5′-OH in **15c′** (see Figures SI.49−53 for NMR characterization of the side product **15c″**). A simple conformational check showed that in compound **15c′** the vicinal C5′ and 6′-*O*- were *cis* to each other with the torsion $\phi_{C5'-C4'-C6'-O6'} = 42°$ (Figure SIII.25). This *cis* comformational disposition made it possible for primary 5′-OH to attack the C=O of the 6′-*O*-(*p*-toluoyl) group to form a relatively stable six-membered carboxonium ion transition state, whereas in compounds **15a′** and **15b′**, $\phi_{C5'-C4'-C6'-O6'}$ was about 75° so formation of such a six-membered transition state was disfavored, and hence no isomeric product was formed owing to migration. Compound **15d′** had the same 6′-*R* configuation as in compound **15c′** and was also accompanied by this type of isomeric side reaction during debenzylation. Fortunately, this side reaction could efficiently

(38) Prakash, T. P.; Puschl, A.; Lesnik, E.; Mohan, V.; Tereshko, V.; Egli, M.; Manoharan, M. *Org. Lett.* **2004**, *6*, 1971–1974.
(39) Varghese, O.; Barman, J.; Pathmasiri, W.; Plashkevych, O.; Honcharenko, D.; Chattopadhyaya, J. *J. Am. Chem. Soc.* **2006**, *128*, 15173–15187.

SCHEME 2

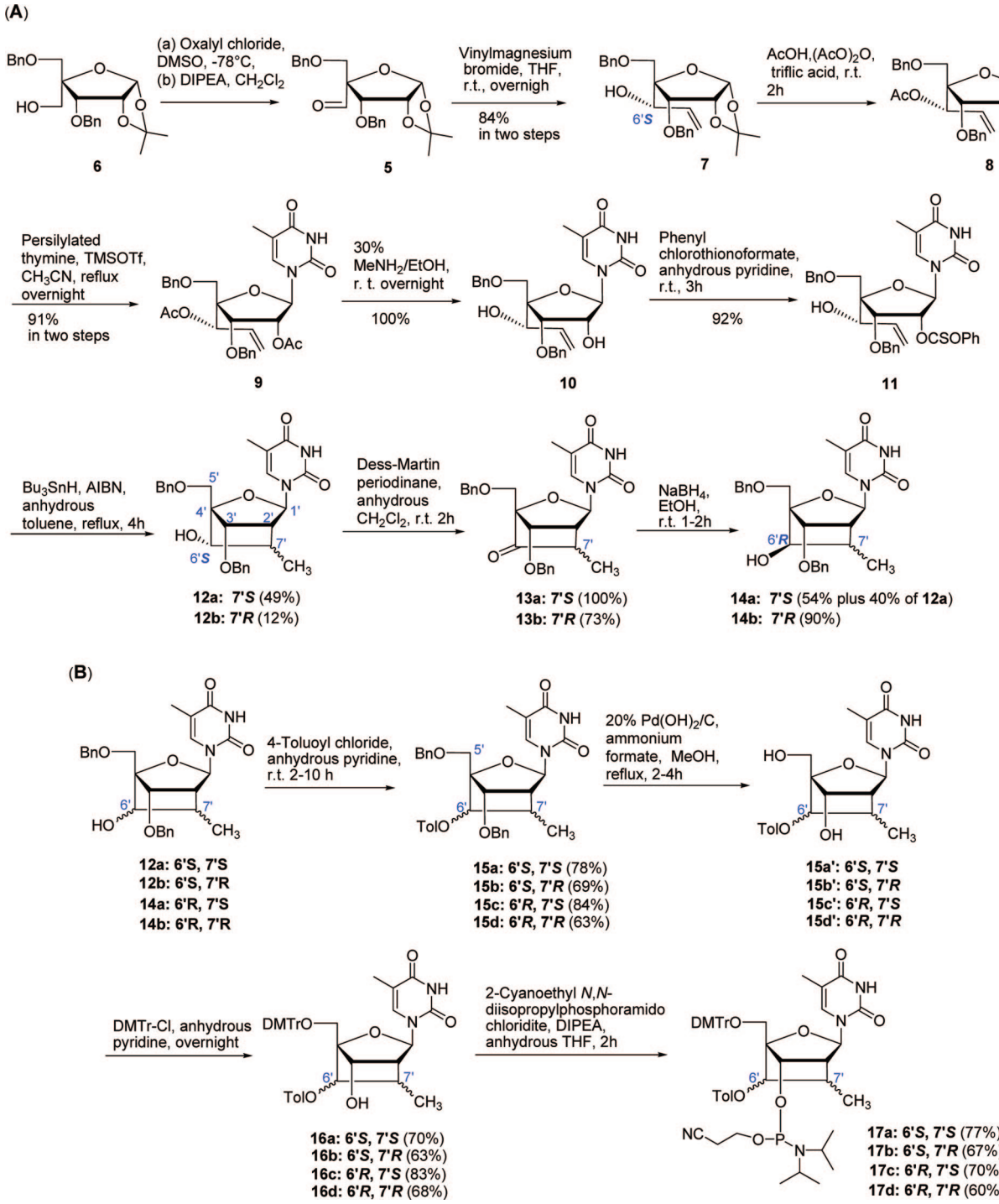

be suppressed by increasing the hydrogenolysis reagents (20% $Pd(OH)_2$/C, 1500 mg/mmol substrate and ammonium formate, 60 equiv). Under this condition, the reaction was completed in a shorter time (2 h) to give pure desired product **15d′**, which could be subjected directly to 5′-dimethoxytritylation to give **16d** in high yield. The 3′-phosphitylation of **16a**−**16d** gave the respective phosphoramidites **17a**−**17d** using standard conditions in moderate yields 60−77%.

For methylation[40] of C6′ of carba-LNA (Scheme 3), the ketone **13a** was treated with methyl magnesium iodide in anhydrous THF for 3 h to give two isomers, **18a** (43%) and **18b** (18%). The two isomers have a large R_f difference on TLC and could easily be separated by short column chromatography. The isomer with lower R_f was the major product, and conformational analysis by 1D NOE (Figure SIII.5) proved it to possess a 6′-*S* configuration (**18a**). The ratio of **18a**/**18b** was 2.5:1, which means attacking the carbon center from the side of the 7′-methyl substituent by methyl anion had more steric hindrance. In view of the stecric hindrance and poorer reactivity of the tertiary 6′-OH, no attempt was made to protect it. Hence, compounds **18a** and **18b** were debenzylated through catalytic hydrogenolysis followed by 5′-dimethoxytritylation to give **19a**

(40) Kakefuda, A.; Yoshimura, Y.; Sasaki, T.; Matsuda, A. *Tetrahedron* **1993**, *49*, 8513–8528.

SCHEME 3

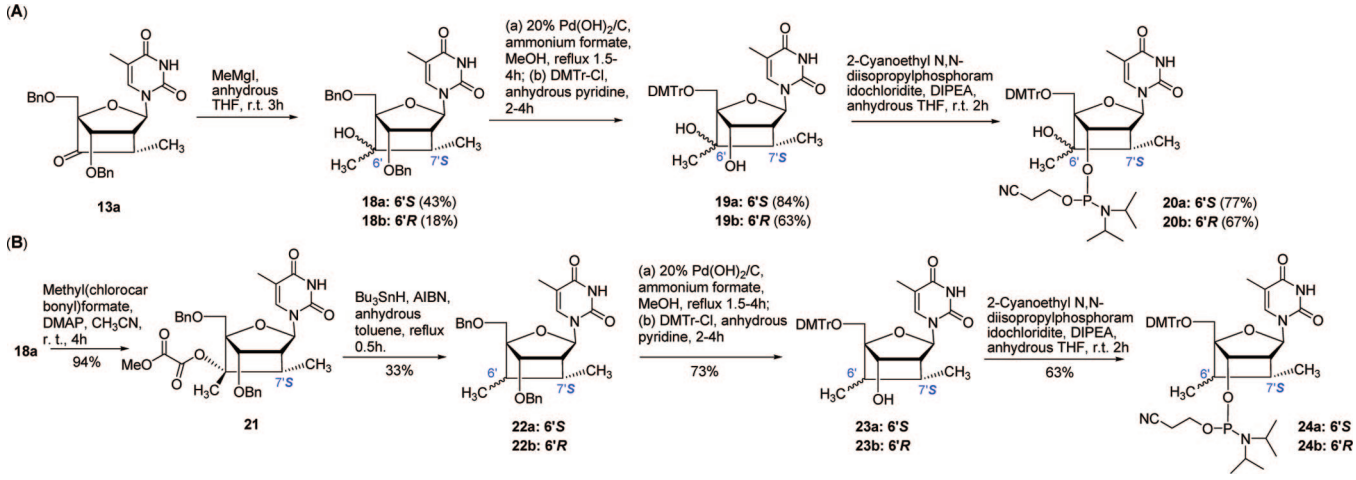

SCHEME 4

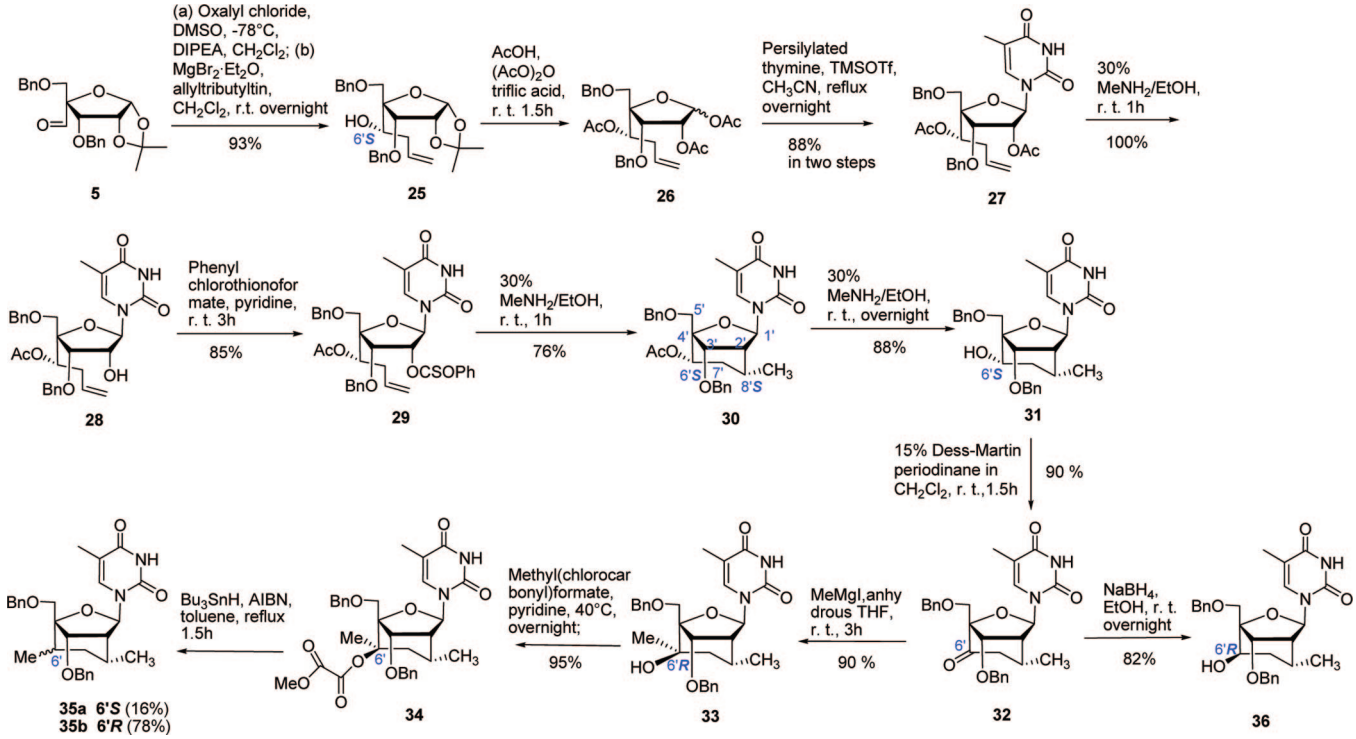

and **19b** in 84% and 63% yields, respectively. Despite the presence of two hydroxyl groups (6′-OH and 3′-OH) in compounds **19a** and **19b**, the 3′-OH could be phosphitylated selectively by treating **19a** and **19b** with 2-cyanoethyl-*N*,*N*-diisopropylphosphoramidochloridite under standard conditions, giving phosphoramidites **20a** and **20b** in 77% and 67% yields, respectively.

To deoxygenate the 6′-OH in compound **18a**, a radical deoxygenation procedure[41] was employed. Thus, **18a** was treated with methyl(chlorocarbonyl) formate[42] in acetonitrile in the presence of DMAP to give **21** in 94% yield. Compound **21** was subjected to a standard radical deoxygenation condition to give an intractable mixture of two isomers **22a** and **22b** (total yield 33%), which could not be separated by column chromatography. The mixture of **22a** and **22b** was debenzylated followed by 5′-dimethoxytritylation to give an intractable mixture of **23a** (6′*S*, 80%)/**23b** (6′*R*, 20%) (total yield 73%), which was phosphitylated to give phosphoramidites **24a** and **24b** as a diastereomeric mixture (63%) that was used directly for DNA synthesis.

The synthetic routes to the modified carba-ENA compounds are shown in Schemes 4 and 5, which are very closely similar to the ones used for the synthesis of carba-LNA derivatives. A brief description of these two schemes, with the detailed experimental procedures, product isolation, and spectroscopic characterization can be found in Supporting Information (SI Part IV).

2. NMR Characterization of Key Intermediates Involved in the Synthesis of the Functionalized Carba-LNA and -ENA Thymidines. All key intermediates **12a/b**, **14a/b**, **18a/b**, **22a/b**, **30**, **31**, **33**, **35a/b**, and **36** were characterized by ^{1}H,

(41) Hartwig, W. *Tetrahedron* **1983**, *39*, 2609–2645.
(42) Dolan, S. C.; MacMillan, J. *J. Chem. Soc., Chem. Commun.* **1985**, 1588–1589.

SCHEME 5

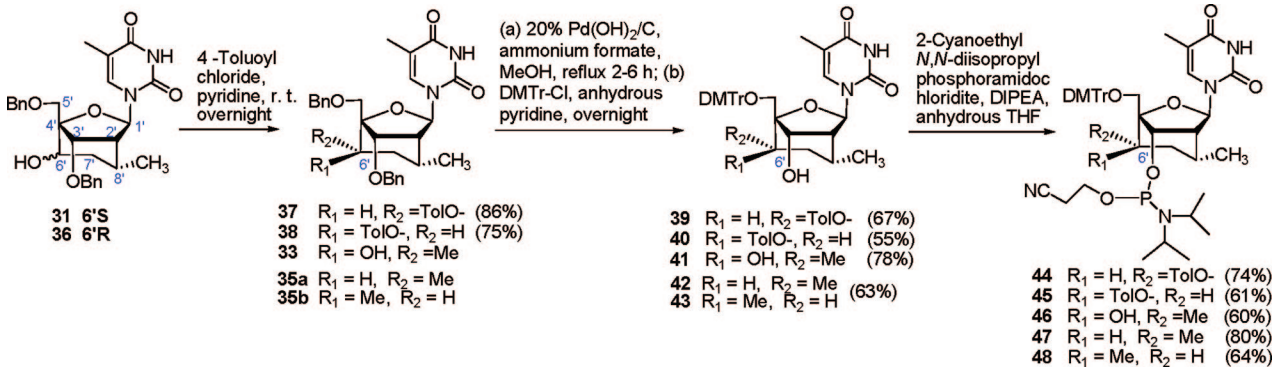

^{13}C, COSY, ^{1}H−^{13}C HMQC, and HMBC NMR and mass spectroscopy.

The correlation between H2′ with H7′ for **12a/b** (Figures SI.11 and SI.16) or H2′ and H8′ for **30** (Figure SII.11) in COSY experiments showed that bicyclic systems have indeed been formed during radical cyclization. This evidence was further corroborated by the observation of long range connectivity of H7′ with C2′ (for compound **12a/b**, Figures SI.13 and SI.18) or H8′ with C2′ (for compound **30**, Figure SII.13) in the HMBC experiments.

The orientation of substituents in carbocyclic moiety of compound **12a/b**, **14a/b**, **18a/b**, **22a/b**, **30**, **33**, **35a/b**, and **36** were assigned by NOE experiments (see Figures SIII.1−SIII.13 and discussion in SI Part IV). The coupling constants were also used to derive information about configurations of various chiral centers in these molecules (Tables SIII.1 and SIII.3). The $^{3}J_{H2',H7'}$ of compounds **12b** and **14b** were close to zero, which suggested that the torsion angles H2′−C2′−C7′−H7′ were nearly 90°, corroborating their 7′*R*-configuration, whereas compounds **12a**, **14a**, **18a/b**, and **22a/b**, which had a $^{3}J_{H2',H7'}$ of ∼4−5 Hz (Figures SIII.14−SIII.21), were in a 7′*S*-configuration. The observation of the four-bond W-coupling (^{w}J) between H3′ and H6′ in compounds **14a/b** (Figures SI.25 and SI.30) and **22b** (Figure SI.96) suggested that the 6′-H point at O4′. The $^{3}J_{H6',H7'}$ in compounds **12a**, **14b**, and **22a** were 8−11 Hz, suggesting that H6′ and H7′ were in *cis* configuration, whereas in compounds **12b**, **14a**, and **22b**, the $^{3}J_{H6',H7'}$ were 3.4−6 Hz (Figures SIII.14−SIII.21), and hence H3′ and H6′ were in *trans* configuration. The carba-ENA adopts a typical chair conformation.[22,28] In compounds **30**, **31**, **33**, **35a**, **35b**, and **36**, the large $^{3}J_{H8',H7''}$ (12−13.5 Hz) suggested that the H8′ and H7″ (axial proton) were in *trans* orientation, and hence the H8′ should also be axial in these compounds. The H6′ in compounds **30**, **31**, and **35a** should also be axial, given the large $^{3}J_{H6',H7''}$ (10.5−12.5 Hz). On the contrary, in compounds **35b** and **36**, H6′ should be equatorial ($^{3}J_{H6',H7''}$ = 7.5 and 5.0 Hz in compounds **35b** and **36**, respectively). Thus the configurational information obtained from coupling constant analysis found to corroborate very well with those obtained from the NOE experiments.

In compounds **19a/b** and **41**, selective phosphitylation at 3′-OH was confirmed by the NMR in that (i) the comparison of the ^{1}H and ^{1}H{^{31}P} NMR spectra showed that the H3′ of compounds **20a/b** and **46** were coupled with ^{31}P with $J\approx$ 10 Hz (Figures SI.80, SI.84, SI 88, SI 91, SII.62, and SII.63), and (ii) the ^{13}C NMR experiment showed the C3′ were also coupled to ^{31}P ($J_{C3',P} \approx$ 15−18 Hz, Figure SI.81 and SI.85) but not to the C6′-Me.

3. Molecular Structures of Functionalized Carba-LNA-T Based on NMR and ab Initio Calculations. Comparison of experimental vicinal coupling constants with those back calculated from the corresponding theoretical torsion angles employing the Haasnoot−de Leeuw−Altona generalized Karplus equation[43,44] have shown satisfactory convergence of the experimental and theoretical results (Table SIII.1). This convergence was a good indicator of the rigidity of both the furanose sugar and the carbocycle moiety of carba-LNA derivatives. The chemical nature and the chirality of the substituents at C6′ and C7′ have been found to dictate the degree of puckering of the constraining 2′,4′ carbocyclic five-membered ring, which has been found to be ranging from near-planar puckering in compound **14b** (C2′−C7′−C6′−C4′ ≈ −0.7°) to nearly 8° for the C2′−C7′−C6′−C4′ torsion in compounds **14a** and **18b** (Table SIII.2). The chemical nature and the chirality of the substituents have also been found to influence puckering of the furanose sugar ring, resulting in the pseudorotational angles ranging from 16° (compound **12b**) to 20° (compound **18b**, Table SIII.2).

4. Thermal Denaturation Studies of Carba-LNA and Carba-ENA Modified AONs 1−52. The phosphoramidites **17a−d**, **20a/b**, **24a/b**, and **44−48** (Schemes 2, 3, and 5) were incorporated into a 15mer DNA sequence through solid-phase DNA synthesis protocol[45] on an automated RNA/DNA synthesizer. The discussion about oligonucleotides synthesis and purification can be found in Supporting Information (SI Part IV). The T_m values of duplexes formed by AONs **1−52** with the complementary RNA or DNA are listed in Table 1. Comparison of T_m's of AONs containing different carba-LNA derivatives clearly suggested how the nature of the modification (-OH versus -CH_3) and their respective stereochemical orientations at C6′ and C7′ in the carbocylic moiety of carba-LNA and carba-ENA modulates the AONs affinity toward the complemenary RNA. This T_m effect owing to -OH versus -CH_3 substitution in the carba moiety gives us an insight as to how the spine of hydration is affected around the internucleotidic phosphate, thereby either minimizing the internucleotidic phosphodirester repulsion or attenuating the stabilization of the phosphate charges through additional salt bridge formation.

4.1. Comparison of Type II with Type III and Type IV with Type V Modifications in Carba-LNA. The [6′*S*-OH,7′*R*-Me]-carba-LNA modified (Type **III**) AONs **10−12** have

(43) Haasnoot, C. A. G.; de Leeuw, F. A. A. M.; Altona, C. *Tetrahedron* **1980**, *36*, 2783–2792.
(44) Altona, C.; Sundaralingam, M. *J. Am. Chem. Soc.* **1972**, *94*, 8205–1822.
(45) Beaucage, S. L.; Caruthers, M. H. *Current Protocols in Nucleic Acid Chemistry*; John Wiley & Sons, Inc.: New York, 2003.

TABLE 1. Thermal Denaturation of Duplexes of Native and Carba-LNA and -ENA Modified AONs with Complementary RNA or DNA[a]

Entry	Modified Carbocyclic structures	Sequence	(MH)$^+$ Cacl.	(MH)$^+$ Found	With RNA T_m	With RNA ΔT_m[c]	With DNA T_m	With DNA ΔT_m[c]
AON 1		3′-d(CTT CTT TTT TAC TTC)	4448.7	4449.7	44.5		45.5	
AON 2	I[b]	3′-d(CT*T* CTT TTT TAC TTC)	4488.7	4489.1	47.0		46.0	
AON 3		3′-d(CTT CT*T* TTT TAC TTC)	4488.7	4489.0	48.5		44.5	
AON 4		3′-d(CTT CTT T*T*T TAC TTC)	4488.7	4489.1	48.5		44.0	
AON 5		3′-d(CTT CTT TTT *T*AC TTC)	4488.7	4489.0	48.0		43.0	
AON 6	II	3′-d(CT*T* CTT TTT TAC TTC)	4504.6	4505.1	47.5	+0.5	47.5	+1.5
AON 7		3′-d(CTT CT*T* TTT TAC TTC)	4504.6	4505.4	49.0	+0.5	48.0	+3.5
AON 8		3′-d(CTT CTT T*T*T TAC TTC)	4504.6	4504.9	49.0	+0.5	47.0	+3.0
AON 9		3′-d(CTT CTT TTT *T*AC TTC)	4504.6	4505.2	48.5	+0.5	44.5	+1.5
AON 10	III	3′-d(CT*T* CTT TTT TAC TTC)	4504.6	4504.5	46.5	-0.5	45.0	-1.0
AON 11		3′-d(CTT CT*T* TTT TAC TTC)	4504.6	4505.0	47.0	-1.5	44.0	-0.5
AON 12		3′-d(CTT CTT T*T*T TAC TTC)	4504.6	4505.1	47.0	-1.5	43.0	-1.0
AON 13		3′-d(CTT CTT TTT *T*AC TTC)	4504.6	4505.2	48.0	0	42.5	-0.5
AON 14	IV	3′-d(CT*T* CTT TTT TAC TTC)	4504.6	4504.8	47.5	+0.5	47.0	+1.0
AON 15		3′-d(CTT CT*T* TTT TAC TTC)	4504.6	4505.4	49.0	+0.5	46.0	+1.5
AON 16		3′-d(CTT CTT T*T*T TAC TTC)	4504.6	4505.1	49.0	+0.5	45.5	+1.5
AON 17		3′-d(CTT CTT TTT *T*AC TTC)	4504.6	4505.5	48.5	+0.5	44.0	+1.0
AON 18	V	3′-d(CT*T* CTT TTT TAC TTC)	4504.6	4504.5	46.0	-1.0	44.5	-1.5
AON 19		3′-d(CTT CT*T* TTT TAC TTC)	4504.6	4504.2	47.0	-1.5	43.0	-1.5
AON 20		3′-d(CTT CTT T*T*T TAC TTC)	4504.6	4503.9	47.0	-1.5	42.5	-1.5
AON 21		3′-d(CTT CTT TTT *T*AC TTC)	4504.6	4503.5	47.0	-1.0	42.0	-1.0
AON 22	VI	3′-d(CT*T* CTT TTT TAC TTC)	4502.7	4502.7	47.0	0	46.0	0
AON 23		3′-d(CTT CT*T* TTT TAC TTC)	4502.7	4502.7	48.0	-0.5	44.0	-0.5
AON 24		3′-d(CTT CTT T*T*T TAC TTC)	4502.7	4502.8	48.0	-0.5	43.5	-0.5
AON 25		3′-d(CTT CTT TTT *T*AC TTC)	4502.7	4503.2	48.0	0	42.5	-0.5
AON 26	VII	3′-d(CT*T* CTT TTT TAC TTC)	4518.6	4518.8	48.5	+1.0	47.5	+1.5
AON 27		3′-d(CTT CT*T* TTT TAC TTC)	4518.6	4518.9	49.0	+0.5	46.5	+2.0
AON 28		3′-d(CTT CTT T*T*T TAC TTC)	4518.6	4518.9	49.0	+0.5	45.5	+1.5
AON 29		3′-d(CTT CTT TTT *T*AC TTC)	4518.6	4519.2	49.0	+1.0	45.0	+2.0
AON 30	VIII	3′-d(CT*T* CTT TTT TAC TTC)	4518.6	4518.4	49.0	+0.5	45.5	+0.5
AON 31		3′-d(CTT CTT T*T*T TAC TTC)	4518.6	4518.8	49.0	+0.5	44.5	+0.5
AON 32		3′-d(CTT CTT TTT *T*AC TTC)	4518.6	4518.0	49.0	+1.0	44.0	+1.0
AON 33	IX[b]	3′-d(CT*T* CTT TTT TAC TTC)	4502.8	4502.1	45.5		44.0	
AON 34		3′-d(CTT CT*T* TTT TAC TTC)	4502.8	4502.3	45.0		40.0	
AON 35		3′-d(CTT CTT T*T*T TAC TTC)	4502.8	4502.2	45.0		40.0	
AON 36		3′-d(CTT CTT TTT *T*AC TTC)	4502.8	4502.3	45.5		40.0	
AON 37	X	3′-d(CT*T* CTT TTT TAC TTC)	4518.8	4518.0	44.5	-1.0	44.0	0
AON 38		3′-d(CTT CT*T* TTT TAC TTC)	4518.8	4518.1	44.0	-1.0	39.5	-0.5
AON 39		3′-d(CTT CTT T*T*T TAC TTC)	4518.8	4518.3	44.0	-0.5	38.0	-2.0
AON 40		3′-d(CTT CTT TTT *T*AC TTC)	4518.8	4518.0	45.5	0	38.5	-1.5
AON 41	XI	3′-d(CT*T* CTT TTT TAC TTC)	4518.8	4518.0	45.5	0	43.5	-0.5
AON 42		3′-d(CTT CT*T* TTT TAC TTC)	4518.8	4518.1	45.5	+0.5	42.2	+2.5
AON 43		3′-d(CTT CTT T*T*T TAC TTC)	4518.8	4517.9	45.5	+0.5	42.0	+2.0
AON 44		3′-d(CTT CTT TTT *T*AC TTC)	4518.8	4518.1	46.0	+0.5	41.0	+1.0
AON 45	XII	3′-d(CT*T* CTT TTT TAC TTC)	4516.8	4515.7	44.5	-1.0	42.5	-1.5
AON 46		3′-d(CTT CT*T* TTT TAC TTC)	4516.8	4516.1	43.5	-1.5	37.5	-2.5
AON 47		3′-d(CTT CTT T*T*T TAC TTC)	4516.8	4516.2	43.5	-1.5	37.0	-3.0
AON 48		3′-d(CTT CTT TTT *T*AC TTC)	4516.8	4516.0	45.0	-0.5	37.0	-3.0
AON 49	XIII	3′-d(CT*T* CTT TTT TAC TTC)	4516.8	4516.0	45.5	0	43.5	-0.5
AON 50		3′-d(CTT CT*T* TTT TAC TTC)	4516.8	4516.1	45.0	0	41.0	+1.0
AON 51		3′-d(CTT CTT T*T*T TAC TTC)	4516.8	4516.0	45.0	0	41.0	+1.0
AON 52		3′-d(CTT CTT TTT *T*AC TTC)	4516.8	4516.2	45.5	0	40.5	+0.5

[a] T_m values measured as the maximum of the first derivative of the melting curve (A_{260nm} vs temperature) in medium salt buffer (60 mM Tris-HCl at pH 7.5, 60 mM KCl, 0.8 mM $MgCl_2$) with temperature range 20 to 70 °C using 1 μM concentrations of the two complementary strands. The value of T_m given is the average of two or three independent measurements. If the error of the first two measurements exceeded ±0.3 °C, the third measurement was carried out to confirm if the error is indeed within ±0.3°C. [b] Modification I and IX have been reported,[28] and here they are standards for comparison. [c] For carba-LNA derivatives modified AONs **6**−**32**, the T_m were compared with (7′-Me)-carba-LNA[28] (Type **I**) modified AONs **2**−**5**, whereas carba-ENA derivatives modified AONs **37**−**52** were compared with (8′S-Me)-carba-ENA[28] (Type **IX**) modified AONs **33**−**36** to give the ΔT_m values.

significantly decreased T_m's (−1.5 to −2°C) compared to [6′*S*-OH,7′*S*-Me]-carba-LNA modified (Type **II**) AONs **6**−**8**, which suggests that when the 7′-methyl group is pointed toward the vicinal 3′-phosphate, it destabilizes the AON/RNA duplex greatly. This result can be further corroborated by the result that [6′*R*-OH,7′*R*-Me]-carba-LNA modified (Type **V**) AONs **18**−**21** also have lower T_m's by −1.5 to −2°C compared to [6′*R*-OH,7′*S*-Me]-carba-LNA modified (Type **IV**) AONs **14**−**17**.

4.2. Comparison of Type II with Type IV and Type III with Type V Modifications in Carba-LNA. [6′*R*-OH,7′*S*-Me]-Carba-LNA modified (Type **IV**) AONs **14**−**17** have similar T_m's as [6′*S*-OH,7′*S*-Me]-carba-LNA modified (Type **II**) AONs **6**−**9**. [6′*R*-OH,7′*R*-Me]-Carba-LNA modified (Type **V**) AONs **18**−**21** have also similar T_m's as [6′*S*-OH,7′*R*-Me]-carba-LNA modified (Type **III**) AONs **10**−**12**, thereby suggesting that the stereochemical orientation of C6′-OH in carba-LNA does not exert a marked effect on the AON/RNA duplex thermal stability.

4.3. Comparison of Type II with Type VII and Type IV with Type VIII modifications in Carba-LNA. Type **VII** ([6′*S*-OH/Me,7′*S*-Me]-carba-LNA) modificaion has one additional C6′-methyl group, which points at the vicinal 3′-phosphate compared to that in Type **II** ([6′*S*-OH,7′*S*-Me]-carba-LNA) modification, and as a result, the Type **VII** modified AONs **26**−**29** have slightly higher (∼0.5 °C) T_m's, at least not less than those in Type **II** modified AONs **6**−**9**. Similarly, [6′**R**-OH/Me,7′*S*-Me]-carba-LNA (Type **VIII**) modified AONs **30**−**32** have similar or slightly higher T_m's compared with those of [6′*R*-OH,7′*S*-Me]-carba-LNA (Type **IV**) modified AONs **30**−**32**. This means that the orientation of the C6′-Me in either *S* or *R* configuration in carba-LNA does not impair the AON/RNA duplex thermal stability, and in some cases, it can even have a stabilization effect.

4.4. Comparison of Type IX with Type X, Type XI, Type XII, and Type XIII Modifications in Carba-ENA. It seems that the hydroxyl and methyl subsitutents in the carbocyclic moiety of carba-ENA exert different kinds of effect on the thermal stability of AON/RNA duplex compared to what is observed in carba-LNAs.

4.4.1. Orientation of C6′-OH in Carba-ENA Plays Important role. In Type **X** modification ([6′*S*-OH,8′*S*-Me]-carba-ENA), C6′-OH points away from the 3′-phosphate, and thus Type **X** modified AONs **37**−**40** have decreased (−1 to −1.5°C) T_m values compared with those in [6′*R*-OH,8′*S*-Me]-carba-ENA modified AONs **41**−**44** in which the C6′-OH points at the 3′-phosphate.

4.4.2. Orientation of C6′-Me in Carba-ENA Is Also Important. [6′*S*-Me,8′*S*-Me]-Carba-ENA modified AONs **45**−**48** give distinctly decreased T_m's compared with those of AONs **33**−**36**, but [6′*R*-Me,8′*S*-Me]-carba-ENA modified AONs **49**−**52** do not have any negative effect on the AON/RNA thermal stability compared to AONs **33**−**36**. This result suggests that when the C6′ methyl group points away from the vicinal 3′-phosphate in carba-ENA, it destabilizes the AON/RNA duplex significantly, but when the C6′ methyl group points at the 3′-phosphate, its role is more subtle.

On the basis of the above comparison, it can be concluded that there are two common features for carba-LNA and -ENA as to how the orientation of hydroxyl and methyl group in the carba moiety influnces the thermal stabliltiy of AON/RNA duplex. First, both the 7′-Me in carba-LNA and 8′-Me in carba-ENA that are located at the center of the minor groove play a marked role in destabilizing the AON/RNA duplex, especially when the methyl group is pointed toward the vicinal 3′-phosphate. The carba-ENA uridine was reported to be stabilizing the AON/RNA duplex by 3.5−4.5 °C/per modification compared to the native counterpart,[22] whereas the (8′-methyl)-carba-ENA thymidine modified AONs **33**−**36** show only 0.5−1°C increase in T_m's. It should be mentioned that the sequences reported here are different from the literature,[22] and so it is not clearly possible here to distinguish the real effect from the sequence-specific effect. Secondly, when the 6′-methyl in carba-LNA or carba-ENA is pointed toward the vicinal 3′-phosphate, it does not impair the thermal stabliltiy of AON/RNA duplex.

The effects on thermal stability of AON/DNA duplex imparted by the carbocyclic substitution follow the same trend as those observed for the AON/RNA duplex, but in general the stabilization or destabilization effect in the AON/DNA homoduplex is more pronounced than in the AON/RNA heteroduplex.

In summary, the electronic and steric influence of substituents and their relative stereochemical configuration in the AON strand on its target RNA affinity is subtle. An additional discussion about how the position and stereochemical orientation of various substitutents on the carbocyclic moiety in the AON strand affects the T_m of the duplex can be found in Supporting Information (SI Part IV).

5. 3′-Exonuclease Stability of the Carbocylic-Modified AONs. New Insights into the Mechanism of the Cleavage. The metabolism of AONs in vivo involves degradation by exo- and endocucleases, and the predominate nuclease activity was of 3′-exonuclease.[46] Here the AONs with a single modification at position ***T***13 (position 3 from 3′-end, see Figure 1D) were chosen to test the 3′-exonuclease resistance of the modified oligonucleotides. Thus, the AONs (^{32}P-labeled at 5′-end) were incubated with phosphodiesterase I from *Crotalus adamanteus* venom (SVPDE) [SVPDE 6.7 ng/μL, AON 3 μM, 100 mM Tris-HCl (pH 8.0), 15 mM $MgCl_2$, total volume 30 μL) at 21°C. Aliquots were taken out at appropriate time intervals and analyzed by 20% denaturing PAGE. The gel pictures obtained upon autoradiography are shown in Figures SIII.24 and SIII.25. The native DNA (**AON 1**) did not show any 3′-exonuclease resistance and was completely degraded in 10 min, whereas for the modified AONs, the last nucleotide T15 was removed quickly to give 14mer oligonucleotides. Because of the presence of ***T***13 modification, phosphate *P*14 (see Figure 1D for phosphate (*P*) numbering) has considerably improved stability toward 3′-exonuclease. ***T***13 modification also improves the stability of the phosphate *P*13 to some extent, so after slow digestion of *P*14, the formed 13mer AON was also relatively stable (see Figures SIII.24 and SIII.25). However, once the *P*13 cleaved, AON was degraded to the monomer blocks quickly, and thus no bands corresponding to 12mer to dimer oligos could be observed.

In Figure 1, total percentages of integrated 14mer and 13mer AONs were plotted against time points to give SVPDE digestion curves for each AON, and pseudo-first-order reaction rates could be obtained by fitting the curves to single-exponential decay functions. A comparison of digestion rates of AONs with different types of modifications showed the following results: (i) 6′-Methyl always considerably improved enzymatic stability of vicinal phosphate linkage. Among the carba-LNA derivatives modified AONs, [6′*R*/*S*-Me,7′*S*-Me]-carba-LNA modified (Type **VI**) AON **22** ($k = 0.0218 \pm 0.0013$ h^{-1}) showed the best

(46) Shaw, J. P.; Kent, K.; Bird, J.; Fishback, J.; Froehler, B. *Nucleic Acids Res.* **1991**, *19*, 747–750.

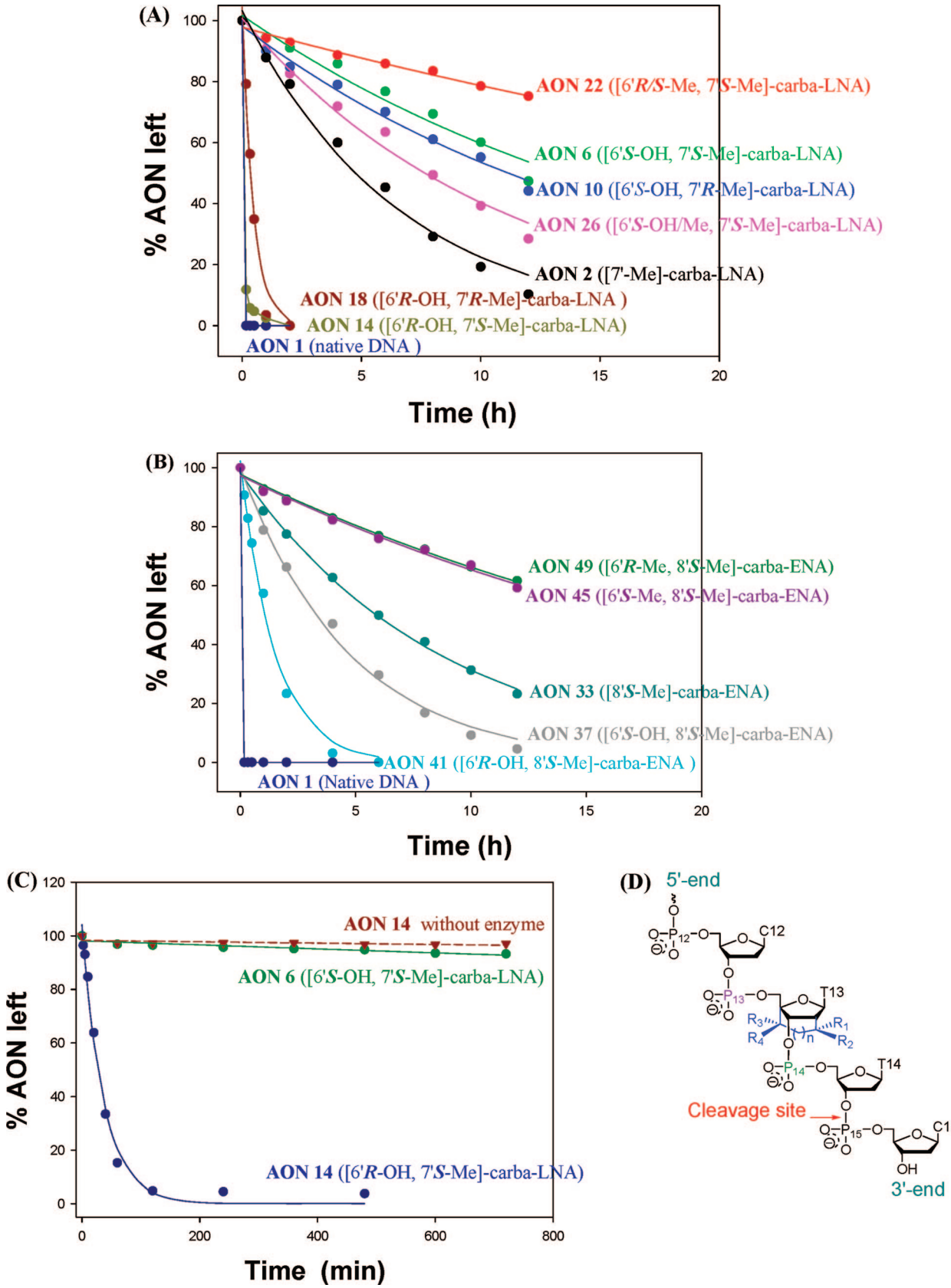

FIGURE 1. Amount of remaining initial oligonucleotide (taken 14mer and 13mer together in %) during 3′-exonuclease (SVPDE) promoted digestion. (A) AONs with functionalized carba-LNA modifications. (B) AONs with functionalized carba-ENA modifications. For panels (A) and (B), following digestion condition was used: AON 3μM (5′-end ^{32}P labeled with specific activity 80 000cpm), 100 mM Tris-HCl (pH 8.0), 15 mM $MgCl_2$, SVPDE 6.7 ng/μL, reaction temperature 21°C, total reaction volume was 30 μL. (C) Comparison of the stabilities of **AON 6** and **AON 14** upon SVPDE digestion using similar digestion condition as in panels A and B, but using lower SVPDE concentration (2.2 ng/μL). (D) Molecular structure of $\underline{T}$13 modified AONs. R_1, R_2, R_3, R_4 = Me, OH or H. n = 0 or 1. The full sequence is 3′-d(CT$\underline{T}^{13}$ CTT TTT TAC TTC-^{32}P)-5′.

enzymatic stability, and was 7 times more stable than [7′-Me]-carba-LNA (Type **I**) modified AON **2** ($k = 0.1525 \pm 0.0097$ h^{-1}); [6′*S*-Me,8′*S*-Me]-carba-ENA (Type **XII**) modified AONs **45** and [6′*R*-Me,8′*S*-Me]-carba-ENA (Type **XIII**) modified AON **49** were also shown to have the best enzymatic stability amongst the carba-ENA derivatives modified AONs. (ii) When 6′-OH pointed at the vicinal 3′-phosphate, it was renderded more susceptible to enzymatic degradation. [6′*R*-OH,7′*S*-Me]-carba-LNA modified (Type **IV**) AON **14** was the least enzymatically stable amongst the carba-LNA modified AONs and was degraded completely in 10 min. The [6′*R*-OH,8′*S*-Me]-carba-ENA (Type **XI**) modified AON **41** ($k = 0.6701 \pm 0.0437$ h^{-1}) was also degraded 6 times faster than the [8′*S*-Me]-carba-ENA (Type **IX**) modified AON **33** ($k = 0.1145 \pm 0.0030$ h^{-1}). (iii) When the 6′-OH pointed away from the vicinal 3′-phosphate, its role was more complex. For example, [6′*S*-OH,8′*S*-Me]-carba-ENA (Type **X**) modified AON **37** ($k = 0.2119 \pm 0.0096$ h^{-1}) was less enzymatically stable than [8′*S*-Me]-carba-ENA modified AON **33**, while [6′*S*-OH,7′*S*-Me]-carba-LNA (Type **II**) modified **AON 6** ($k = 0.0532 \pm 0.0044$ h^{-1}) and [6′*S*-OH,7′*R*-Me]-carba-LNA (Type **III**) modified AON **10** ($k = 0.0605 \pm 0.0032$ h^{-1}) were 2−3 times more stable than [7′-Me]-carba-LNA modified AON **2**. One interesting observation is that when the 6′-OH points away from the vicinal 3′-phosphate (C6′-*S*), as in modifications **II**, **III**, **VII**, and **V** in AON **6**, **10**, **26**, and **37**, it can improve the nuclease resistance of 5′-phosphate (*P*13 in Figure 1D) and so the band corresponding to 13mer could be observed on PAGE. (iv) By comparing degradation kinetics and digestion pattern of [6′*R*-OH,7′*S*-Me]-carba-LNA modified (Type **IV**) AON **14** with [6′*R*-OH,7′*R*-Me]-carba-LNA modified (Type **V**) AON **18**, [6′*S*-OH,7′*S*-Me]-carba-LNA modified (Type **II**) AON **6** with [6′*S*-OH,7′*R*-Me]-carba-LNA modified (Type **III**) AON **10**, it could be concluded that the 7′-methyl, when it pointed at the vicinal 3′-phosphate (C7′-*R*), had more positive effect on the enzymatic stability of the vicinal 3′-phosphate than when it pointed away from(C7′-*S*) the phosphate. (v) Comparing digestion rates (Figure SIII.26) of carba-LNA modifications with carba-ENA modifications that have the same substitution (same fuctional group, location and orientation), it could be seen that although carba-ENA derivatives have an additional endocyclic methylene group, they did not show significantly better nuclease resistance compared to that of the carba-LNA counterparts.

5.1. Lipophilic Substituents Improve Exonuclease Resistance of the Vicinal Scissile Phosphate, Depending upon Their Stereochemical Orientation with Respect Vicinal Phosphate. The most interesting conclusion one can derive from the above results is that the exonuclease resistance is dependent not only on the lipophilic *versus* hydrophilic nature of the substituent but also significantly on the stereochemical orientation of its chirality vis-à-vis scissile phosphate. In our previous study,[28] comparison of nuclease resistance of different 2′,4′-constrained modifications with different lipophilic or hydrophilic nature of the C2′-substituent (oxo vs aza vs carba) led to the conclusion that hydration around the C2′-substituent was an important factor for promoting the nuclease-promoted hydrolysis of phosphate. That study showed that the lipophilic C2′ carba-substituent can improve the nuclease resistance of the vicinal scissile phosphate. In the present study, this conclusion was further corroborated by the fact that the methyl substitution in the carbocycle moiety of the carba-LNA or -ENA, independent of its location, can always improve nuclease resistance of AONs. The lipophilic nature of the methyl group conferred nuclease resistance by two effects: First, the methyl could decrease the magnitude of hydration around the scissile phosphate (hydrophobic effect). Second, the bulky methyl could also disturb the interaction between nuclease and phosphate linkage owing to the steric clash. This effect was also illustrated by Imanishi's group recently.[23] All of the modifications of Type **II**, **III**, **IV**, and **V** in AONs **6**, **10**, **14**, and **18** have a 7′-methyl substituent, but [6′*S*-OH,7′*R*-Me]-carba-LNA modified (Type **III**) AON **10** and [6′*R*-OH,7′*R*-Me]-carba-LNA modified (Type **V**) **18** were more stable than [6′*S*-OH,7′*S*-Me]-carba-LNA modified (Type **II**) AON **6** and [6′ ***R***-OH,7′*S*-Me]-carba-LNA modified (Type **IV**) **14**, respectively (if only the stability of *P*14 is considered, see Figure SIII.27). This result suggested that as the scissile phosphate came closer to the lipophilic substituent, it became more stable toward the nuclease degradation. Thus, the case that carba-ENA do not have significantly improved nuclease resistance compared to carba-LNA could be plausibly explained by the fact that the six-membered carbocycle of carba-ENA adopted a perfect chair conformation,[22,47] and thus the additional endocyclic methylene group orientated away from the 3′-phosphate (see the model in Figure SIV.4). On the contrary, an additional methyl group at C6′ of carba-LNA, which is spatially located at the edge of the minor groove, came much closer to the vicinal scissile phosphate linkage, resulting in its greater improvement in the nuclease stability.

5.2. Studies on a Pair of Pure Diastereomers of C6′-Hydroxyl (*R* and *S*)-Substituted Carba-LNA Shows the Chirality-Dependent Stabiliy of the Scissile Phosphate toward Exonuclease. Hydroxyl substitution on the carbocyclic moiety generally leads to loss of enzymatic stability of vicinal phosphate, as expected from the above discussion. Thus, AONs **37** and **41** with the hydrophilic 6′-OH substituents are less enzymatic stable than the unsubstituted AON **33**. Similarly, AONs **14** and **18** are less enzymatically stable than AON **2** (see Figure 1A and B). The orientation of hydrophilic 6′-OH had even more pronounced effect on the nuclease resistance of the vicinal scissile phosphate. The 6′-OH in [6′*S*-OH,7′*S*-Me]-carba-LNA (Type **II**) modified AON **6** and [6′*R*-OH,7′*S*-Me]-carba-LNA modified (Type **IV**) AON **14** orientate with opposite chirality. As a result, AON **6** and AON **14** had completely different stability toward SVPDE incubation. In the upper experiment, AON **14** with 6′-OH pointing toward the 3′-phosphate was degraded so fast that no accurate degradation rate could be obtained. Hence, AON **6** and **14** were incubated under a very low concentration of SVPDE [SVPDE 2.2 ng/μL, AON 3μM, 100 mM Tris-HCl (pH 8.0), 15 mM $MgCl_2$, 21°C, total volume 30 μL]. The gel pictures obtained by autoradiography are shown in Figure SIII.28, and the degradation curves are shown in Figure 1C. Under this condition, AON **6** ($k = 0.0001$ min^{-1}), with modification Type **II** in which 6′-OH pointed away from the 3′-phosphate (C6′-*S*, $d_{6'O-P} \approx 5.5$ Å, the molecular model is shown in Figure SIV.2) is 270 times more stable than AON **14** ($k = 0.027 \pm 0.0019$ min^{-1}) with modification **IV** in which C6′-OH pointing toward the 3′-phosphate (C6′-*R*, $d_{6'O-P} \approx 4.4$ Å). On the other hand, if AON **14** was incubated in the same buffer but without enzyme, it was totally stable. This result ruled out any possibility that a pH 8.0 buffer used in the SVPDE digestion can mediate any

(47) Zhou, C.; Plashkevych, O.; Chattopadhyaya, J. *Org. Biomol. Chem.* **2008**, Epub ahead of print; DOI: 10.1039/B813870B.

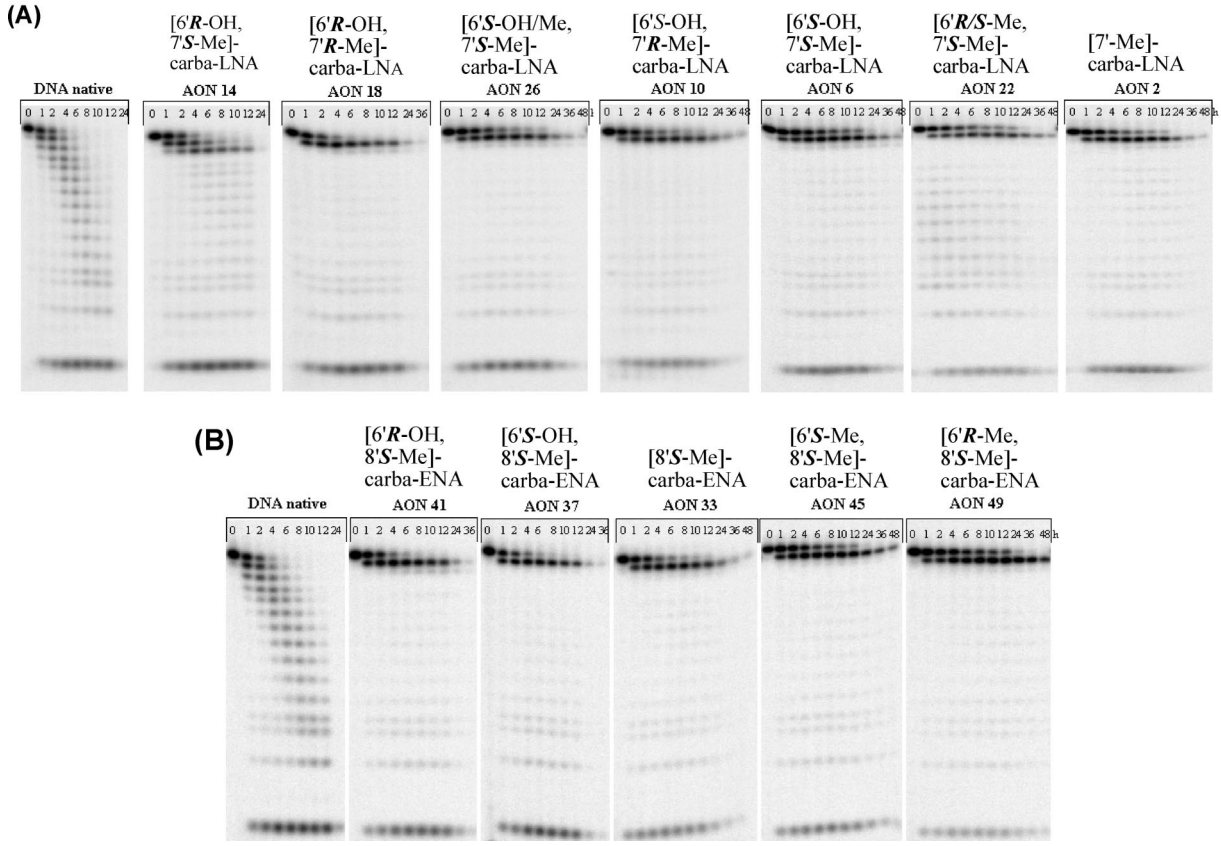

FIGURE 2. Autoradiograms of 20% denatured PAGE showing the stability of 5′-^{32}P-labeled AONs in human blood serum. (A) Carba-LNA derivatives modified AONs. (B) Carba-ENA derivatives modified AONs.

cleavage of phosphate in Type **IV** modified AON **14** by intramolecular transesterification.

6. Stability of Carba-LNA and -ENA Modified AONs in Human Blood Serum. Blood serum stability of AONs with a single modification at position ***T***13 (Table 1) has also been tested. The AONs (^{32}P-labeled at 5′-end) were incubated with human blood serum (male, Type AB) up to 48 h at 21°C and aliquots were taken out at regular time intervals and analyzed by 20% denaturing PAGE. The gel pictures obtained by autoradiography are shown in Figure 2. Because of the presence of alkaline phosphatase in serum that removed the 5′-end ^{32}P-label gradually, it was impossible to get the quantified data from the gel picture to compare their relative blood serum stability. Comparison of the gel pictures shows that the [6′*S*-OH,7′*S*-Me]-carba-LNA modified (Type **II**) AONs **6**, [6′*S*-OH,7′*R*-Me]-carba-LNA modified (Type **III**) AON **10**, [6′*R*/*S*-Me,7′*S*-Me]-carba-LNA modified (Type **VI**) AON **22**, and [6′*S*-OH/Me,7′*S*-Me]-carba-LNA modified (Type **VII**) AON **26** were more stable than [7′-Me]-carba-LNA modified (Type **I**)[28] AON **2** in blood serum, whereas [6′*R*-OH,7′*S*-Me]-carba-LNA modified (Type **IV**) AONs **14** and [6′*R*-OH,7′*R*-Me]-carba-LNA modified (Type **III**) AON **18** were much less stable than AON **2** upon blood serum treatment. For AONs containing carbocylic-ENA derivatives, their relative stabilities in human blood serum were as follows: [6′*R*-Me,8′*S*-Me]-carba-ENA modified AON **49**, [6′*S*-Me,8′*S*-Me]-carba-ENA modified AON **45** > [8′*S*-Me]-carba-LNA modified AON **33** > [6′*S*-OH,8′*S*-Me]-carba-ENA modified AON **37**, [6′*R*-OH,8′*S*-Me]-carba-ENA modified **41** > native DNA. Comparison of all modified craba-LNA and carba-ENA modified AONs, however, showed that the carba-ENA modified AON **49** is more stable than all other AONs reported here (Figure 2). It therefore appeared that in human blood serum the relative order of stability of modified AONs was nearly the same as that found upon treatment with 3′-exonuclease.

7. Lessons from Modifications in the AON versus Target Affinity vis-à-vis Nuclease Resistance. From combination of the target affinity and nuclease resistance of modified AONs **2**−**52**, the following conclusions can be obtained: (i) In the center of the minor groove, hydrophobic and steric modification is not favored. This type of modification causes obvious loss of target affinity toward RNA. (ii) At the edge of the minor groove, hydrophobic and steric modification are attractive in that this type of modification can result in considerable improvement on enzymatic stability, at the same time without loss of target affinity. (iii) Hydrophilic modification close to phosphate linkage makes the phosphate too labile toward the nuclease, and so this type of modification should be avoided.

For AONs with [6′*S*-OH,7′*S*-Me]-carba-LNA (Type **II**) and [6′*S*-OH/Me,7′*S*-Me)-carba-LNA (Type **VII**) modifications, their affinity toward complementary RNA (T_m, +4 to +5 °C/modification compared to the native counterpart) are similar to that of AONs that have LNA modification (T_m, +5°C/modification under the same conditions).[28] At the same time, they are enzymatically 2−3 times more stable than AONs with the [7′-Me]-carba-LNA (Type **I**) modification, which are known to be much more stable than LNA modified AONs.[28] Hence, Type **II** and **VII** modified AONs are deemed to be excellent candidates for antisense therapeutics.

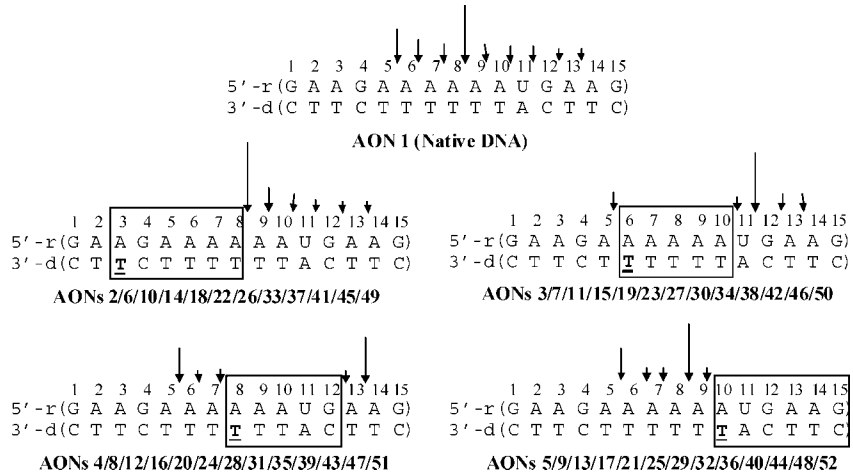

FIGURE 3. *Escherichia coli* RNase H1 promoted cleavage pattern of AONs **1**−**52**/RNA duplexes. Vertical arrows show the RNase H cleavage sites, with the relative length of the arrow showing the extent of the cleavage. The square boxes show the stretch of the modification, which is resistant to RNase H1 cleavage, thereby giving footprints.

8. RNase H Activity of Carba-LNA and -ENA Modified AONs with the Complementary RNA Is Very Similar to That of the Native Counterpart. In the antisense strategy, RNase H recruitment is a very important property when the modified AONs are bound to the target RNA in heteroduplex form. The [7′-methyl]-carba-LNA and [8′*S*-methyl]-carba-ENA were reported to be able to elicit RNase H activity and the relative RNA cleavage rates were very similar to that of the native counterpart.[28] It was known that RNase H binds to the DNA/RNA hybrid in the minor groove.[48] In the present study, all of the modified compounds have their substituents located in the minor groove and so are ideal substrates to illustrate how the lipophilic versus hydrophilic or steric nature of the substituents in the modified AONs affects the efficiency of RNase H elicitation. Hence, native AON **1** and all of the modified AONs **2**−**52** were hybridized with 5′-^{32}P labeled 15mer complementary RNA at 21 °C and incubated with *Escherichia coli* RNase H1. Aliquots were taken after 5, 10, 15, 30, and 60 min and analyzed by denaturing PAGE. The results are shown in Fig SIII.29.

All modified AONs **2**−**52**/RNA hybrids were found to be excellent substrates for RNase H. The cleavage pattern was not affected by the nature of different substituents but depended upon the site of the modification. For example, despite the fact that all AONs **6/10/14/18/22/26/33/37/41/45/49** have different substituents in the carbocyclic moiety at position 3 from the 3′-end, they showed cleavage patterns similar to those of [7′-Me]-carba-LNA (Type **I**) modified AON **2** and [8′*S*-Me]-carba-ENA (Type **IX**) modified AON **33** (Figure 3). For all of the modified AONs **2**−**52**, the cleavage activity of RNase H was suppressed within a 4−5 base pairs long region that starts from the base opposite the modified **T** nucleotide, towards the 3′-end of the RNA strand. The RNase H promoted cleavage has a preference at the middle site A8 of the RNA strand for native AON **1**/RNA duplex. If A8 is included within the suppressed region, the major cleavage site shifts to the edges of the suppressed region.

The cleavage rates were determined by autoradiography of gels and subsequently by plotting the uncleaved RNA fraction as a function of time (Figure SIII.29). Fitting the degradation curves to single-exponential decay functions gave the reaction rates that are shown as bar plots (Figure 4). The main observations are as follows: (i) cleavage rate is site-dependent. Exclusively, the AONs/RNA having the modification at positions 6 and 8 from the 3′-end in the AON strands have lower cleavage rates. Moreover, AONs with the modification at position 8 generally give the lowest degradation rates. On the contrary, cleavage rates for AONs/RNA with modification at the positions 3 and 10 from the 3′-end of the AON strands generally were similar to or even faster than that of the native counterpart. (ii) Cleavage efficiency is not very sensitive to the nature of substituents in the carbocyclic moiety especially for the carba-ENA derivatives. Cleavage of RNA in AONs **37**−**52**/RNA was as efficient as the cleavage of RNA in AONs **33**−**36**/RNA. For carba-LNA derivatives, [6′*S*-OH,7′*S*-Me]-carba-LNA (Type **II**) modfied AONs **6**−**9**, [6′*S*-OH,7′*R*-Me]-carba-LNA (Type **III**) modified AONs **10**−**13**, and [6′*S*-OH/Me,7′*S*-Me]-carba-LNA (Type **VII**) modified AONs **26**−**29** elicit slightly less recruitment of RNase H.

For cleavage of AON/RNA hybrids by RNase H, the cleavage footprint pattern is affected primarily by the global conformation of AON/RNA hybrid. AONs containing 2′,4′-bridged modification, such as LNA, carba-LNA, aza-ENA, and carba-ENA, generally showed identical cleavage footprint patterns.[28] This is presumably caused by the local conformational change imparted by the constrained nature of the modifications. This conformational change leads to a stretch of ca. 5 bp, starting from the modification site toward the 5′-end in the AON strand, not accessible to RNase H. In the present study, all of the modified AON/RNA hybrids have shown a similar cleavage pattern, suggesting that the hydroxyl or methyl substitution in the carbocyclic moiety of carba-LNA and carba-ENA does not lead to significant conformational disruption.

In the native AON **1**/RNA hybrid, the RNase H1 cleavage between position 5 and position 13 from the 5′-end of the RNA strand and have a strong preference at position 8 (Figure 3). However, if position 8 is included in the stretch of modification, a new preferred cleavage site appeared in the end of the modification stretch. Though the sequence in the new preferred cleavage site is different from that at position 8, this sequence difference should contribute limitedly to cleavage rate variation

(48) Zamaratski, E.; Pradeepkumar, P. I.; Chattopadhyaya, J. *J. Biochem. Biophys. Methods* **2001**, *48*, 189–208.

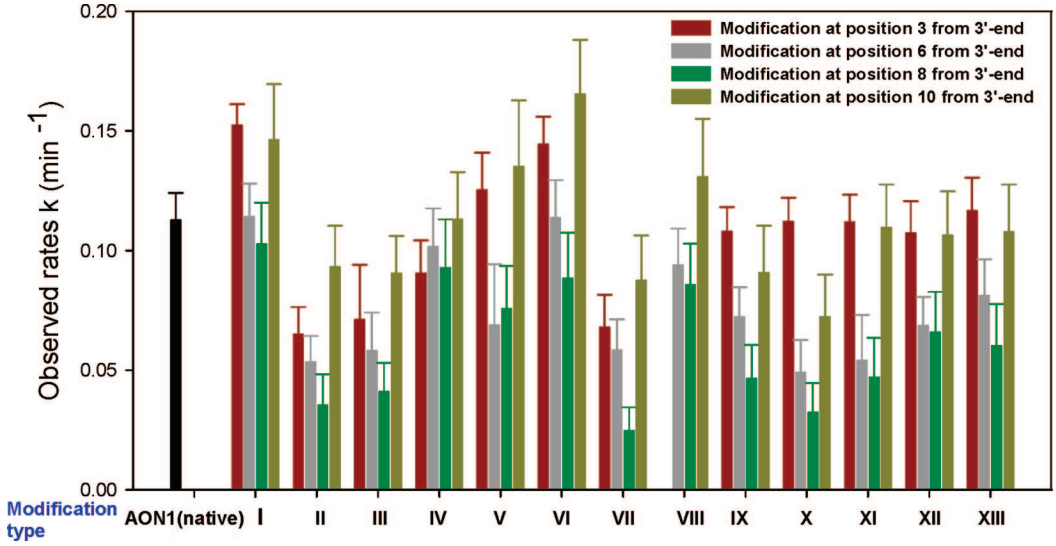

FIGURE 4. Bar plots of the observed cleavage rates of the RNase H1 promoted degradation of RNA in AON **1**−**52**/RNA hybrid duplexes. The degradation curves are shown in Figure SIII.33.

because RNase H1 only displays minimal sequence preference.[49,50] The observation that AONs with the modification at position 6 and especially at position 8 gave much lower degradation rates by RNase H1 (see Figure 4) suggests that if the original preferred cleavage site is located in the stretch of modification, the RNA degradation rates by RNase H1 will be affected.

Conclusions

1. To study how the fine modulation around the phosphodiester moiety in the AON can affect its antisense property such as target affinity, nuclease resistance, and RNase H elicitation, carba-LNA and carba-ENA with hydroxyl and/or methyl substituents attached at the carbocyclic moiety were synthesized. Various NMR experiments including ^{1}H, ^{13}C, DEPT, one bond ^{1}H−^{13}C correlation (HMQC), and long range ^{1}H−^{13}C HMBC experiments have been employed to characterize all synthesized compounds. The configuration of subsituents in the key intermediates was determined by NOE and was also corroborated by the $^{3}J_{H,\ H}$ coupling constants obtained from ^{1}H homodecoupling experiments as well as by *ab initio* calculations.

2. The relationship between substitution and target affinity and nuclease resistance of AONs can be summarized as follows: (i) In the center of the minor groove, the hydrophobic and steric substituents are not favored. This type of modification decreases the AON′s target affinity obviously but without significant improvement on the nuclease resistance. (ii) Steric substitution on the edge of the minor groove is favored. Modified AONs with these substituents retain the improved target affinity that carbocyclic LNA/ENA provide and have much better nuclease resistance. At the same time, they do not cause any loss of RNase H elicitation. (iii) Hydrophilic modification close to the internucleotide phosphate linkage should be avoided because it makes AONs especially enzymatically unstable. These conclusions confirm the importance of the chemical characteristics of the substituent-type such as lipophilic vs hydrophobic. They also highlight the key role of stereochemical orientation of the substituents in the minor groove of the heteroduplex in engineering the antisense properties of the carba-modified AONs.

3. For the RNase H1 mediated RNA cleavage in an AON/RNA hybrid, the cleavage pattern and rate is not very sensitive to the nature of substitution in the carbocyclic moiety of the carba-LNA and carba ENA. The RNase H has strong positional preference for a given active DNA/RNA hybrid. During design of the modified antisense oligonucleotides by gapmer technology, in order to ensure high cleavage efficiency by RNase H, the original preferred cleavage site in the stretch of modification should be avoided.

4. Type **II** and **VII** modified AONs have better target affinity and nuclease stability than the Type **I** carba-LNA. In addition, Type **II** and **VII** modified AONs can also elicit RNase H activity efficiently, which make them excellent candidates as potential antisense or RNAi therapeutic agents.

Experimental Section

Note: All individual reaction steps, work-up, and product characterization for compounds **13b**, **14b**, **15b**−**d**, **16b**−**d**, **17a**−**d**, **19a/b**, **20a/b**, **23a/b**, **24a/b**, and **25**−**48** are given in Supporting Information (SI Part IV).

3,5-Di-*O*-benzyl-4-*C*-(1-hydroxy-allyl)-1,2-*O*-isopropylidene-α-D-ribofuranose (7). Oxalyl chloride (4.1mL, 46 mmol) was added to precooled CH_2Cl_2 (1200 mL) at −78 °C. Then DMSO (5.3 mL, 74 mmol) was added dropwise to the solution over 30 min. After stirring for 20 min, a solution of **6** (7.4 g, 18.5 mmol) in CH_2Cl_2 (35 mL) was added dropwise over about 20 min, and the mixture was kept stirring at −78 °C for another 30 min. Then reaction was cooled with ice, and DIPEA (22 mL) was added. The mixture was then allowed to warm to room temperature, and water was added. The organic layer was separated, washed with water and brine, dried over $MgSO_4$, and concentrated under reduced pressure to give the corresponding aldehyde **5** as oil. This oil was dissolved in THF (220 mL) under nitrogen and cooled to 0 °C. Vinylmagnesium bromide (1.0 M solution in THF, 39 mL, 37 mmol) was added, and then it was allowed to warm to room temperature and kept stirring at this temperature overnight. The reaction was quenched with water (600 mL) slowly. After recovery of THF, the residue was diluted with CH_2Cl_2, washed with saturated $NaHCO_3$, dried

(49) Crooke, S. T.; Lemonidis, K. M.; Neilson, L.; Griffey, R.; Lesnik, E. A.; Monia, B. P. *Biochem. J.* **1995**, *312*, 599–608.
(50) Wu, H.; Lima, W. F.; Crooke, S. T. *J. Biol. Chem.* **1999**, *274*, 28270–28278.

over $MgSO_4$, and concentrated under reduced pressure. The crude material was purified by column chromatography on silica gel (0−5 % ethyl acetate in cyclohexane, v/v) to give **7** as a colorless oil (7.1 g, 84%). ^{1}H NMR (600 MHz, $CDCl_3$): δ 7.4−7.2 (10H, m, Bn), 6.05 (1H, m, H7), 5.81 (1H, d, $J_{H1,\ H2}$ = 4.2 Hz, H1), 5.37 (1H, dd, J = 2.4 Hz, 17.4 Hz, H8), 5.19 (1H, dd, J = 2.4 Hz, 11.4Hz, H8), 4.98 (1H, m, H6), 4.87(1H, d, J_{gem} = 11.4 Hz, C$\underline{H}_2$Bn), 4.70 (1H, dd, $J_{H1,H2}$ = 4.2 Hz, $J_{H2,H3}$ = 5.4 Hz, H2), 4.50 (2H, dd, J_{gem} = 11.4 Hz, 11.4Hz, C$\underline{H}_2$Bn), 4.47 (1H, d, $J_{H3,H2}$ = 5.4 Hz, H3) 4.37 (1H, d, J_{gem} = 11.4 Hz, C$\underline{H}_2$Bn), 3.76 (1H, d, J_{gem} = 10.8 Hz, H5), 3.56 (1H, m, 6-OH), 3.52 (1H, d, J_{gem} = 10.8 Hz, H5), 1.60 (3H, s, C$\underline{H}_3$), 1.36 (3H, s, C$\underline{H}_3$); ^{13}C NMR (150 MHz, $CDCl_3$): δ 139.9 (Bn), 138.7 (Bn), 137.0 (C7) 130.4, 130.1, 129.8, 129.3 (aromatic), 117.0 (C8), 115.0 (isopropyl), 106.7 (C1), 88.9 (C4), 80.7 (C2), 80.4 (C3), 75.3 (C$\underline{H}_2$Bn), 74.7 (C$\underline{H}_2$Bn), 73.9 (C6), 71.1 (C5), 28.6 (C$\underline{H}_3$), 28.2 (C$\underline{H}_3$). MALDI-TOF *m*/*z*: $[M + Na]^+$ 449.1, calcd 449.2.

1-[4-*C*-(1-Acetyl-allyl)-2,6-di-*O*-acetyl-3,5-di-*O*-benzyl-β-D-ribofuranosyl]-thymine (9). Acetic anhydride (36 mL, 380 mmol) and acetic acid (175 mL) were added to **7** (12.5 g, 29 mmol). The mixture was cooled, and triflic acid (0.2 mL, 1.4 mmol) was added. After stirring for 2 h at room temperature, the reaction was quenched with cold saturated $NaHCO_3$ solution and extracted with CH_2Cl_2. The organic layer was separated, dried over $MgSO_4$, and evaporated to give crude product **8**, which was coevaporated with anhydrous CH_3CN thrice and dissolved in the same solvent. Thymine (4.31 g, 34 mmol) and *N*,*O*-bis(trimethylsilyl)acetamide (16 mL, 65 mmol) were added to the solution and refluxed for 45 min until the suspension became a clear solution. Then reaction mixture was cooled to 0 °C, and TMSOTf (6.18 mL, 34 mmol) was added dropwise, followed by reflux overnight. CH_3CN was evaporated under reduced pressure. To the residue was added saturated NH_4Cl solution and the mixture was extracted with CH_2Cl_2. The organic layer was dried with $MgSO_4$, evaporated, and chromatographed over silica gel (1−3 % methanol in CH_2Cl_2, v/v) to give **9** as a white foam (14 g, 24 mmol, 91%). ^{1}H NMR (270 MHz, $CDCl_3$): δ 8.73 (1H, s, N$\underline{H}$), 7.42 (1H, s, H6), 7.22−7.35 (10H, m, Bn), 6.31 (1H, d, $J_{H1',H2'}$ = 6.56 Hz, H1′), 5.94 (1H, m, H7′), 5.79 (1H, d, $J_{H6',H7'}$ = 4.80 Hz, H6′), 5.48 (1H, app t, J = 6.31 Hz, 12.0 Hz, H2′), 5.14−5.28 (2H, m, H8′), 4,52 (5H, m, 2 x C$\underline{H}_2$Bn, H3′), 3.76 (2H, s, H5′, H5″), 2.04 (3H, s, acetyl-C$\underline{H}_3$), 1.90 (3H, s, acetyl-C$\underline{H}_3$), 1.47 (3H, s, T-C$\underline{H}_3$). ^{13}C NMR (67.5 MHz, $CDCl_3$): δ 170.4 (C$\underline{=}$O, acetyl), 168.6 (C$\underline{=}$O, acetyl), 163.5 (C4), 150.5 (C2), 137.0 (aromatic), 135.7 (C6), 132.0 (C7′), 128.8, 128.6, 128.2, 128.1,127.8, 127.6 (aromatic), 117.6 (C5), 111.6, (C8′), 88.0 (C4′), 87.0 (C1′), 79.1 (C3′), 75.3 (CH_2Bn), 75.0 (C2′), 74.0 (C$\underline{H}_2$Bn), 72.9 (C6′), 72.1 (C5′), 20.8 (acetyl-C$\underline{H}_3$), 20.7 (acetyl-C$\underline{H}_3$), 12.0 (T-C$\underline{H}_3$). MALDI-TOF *m*/*z*: $[M + H]^+$ 579.2, calcd 579.2.

1-[3,5-Di-*O*-benzyl-2,6-di-hydorxy-4-*C*-(1-hydroxy-allyl)-β-D-ribofuranosyl]-thymine (10). Compound **9** (6.9 g, 12 mmol) was treated with 30% methylamine solution in ethanol (240 mL) at room temperature overnight. Then reaction mixture was extracted with CH_2Cl_2, washed with $NaHCO_3$ solution, and dried over $MgSO_4$. After evaporation of solvent, the residue was chromatographed over silica gel (0−2.5 % methanol in CH_2Cl_2, v/v) to give **10** (6.8 g, 100%) as a white solid. ^{1}H NMR (600 MHz, $CDCl_3$): δ 9.92 (1H, s, N$\underline{H}$), 7.55 (1H, s, H6), 7.26−7.36 (10H, m, Bn), 6.08 (1H, d, $J_{H1',H2'}$ = 5.4 Hz, H1′), 5.94 (1H, m, H7′), 5.32(1H, dt, $J_{H7',H8'}$ = 17.4 Hz, H8′), 5.19(1H, dt, $J_{H7',H8''}$ = 10.6 Hz, H8″), 5.01 (1H, d, C$\underline{H}_2$Bn), 4.71 (1H, m, H6′), 4.70 (1H, d, C$\underline{H}_2$Bn), 4.52 (3H, s, H2′, C$\underline{H}_2$Bn), 4.40 (1H, d, $J_{H2',H3'}$ = 5.4 Hz, H3′), 3.80(1H, d, J_{gem} = 10.8 Hz, H5′), 3.66(1H, d, J_{gem} = 10.8 Hz, H5″), 2.89 (d, 1H, J = 4.2 Hz, OH), 1.47(3H, s, T-C$\underline{H}_3$). ^{13}C NMR (150 MHz, $CDCl_3$): δ 163.9 (C4), 151.3 (C2), 137.4, 137.2, 135.9, 135.3, 128.81, 128.7, 128.4, 128.3, 128.1, 127.6, 116.2, 111.0 (C5), 89.4 (C1′), 87.7 (C4′), 79.4 (C3′), 75.3 (C2′), 74.7 (Bn), 73.8 (Bn), 72.6 (C6′), 70.5 (C5′), 12.10 (T-C$\underline{H}_3$). MALDI-TOF *m*/*z*: $[M + Na]^+$ 517.2, calcd 517.2.

1-[3,5-Di-*O*-benzyl-4-*C*-(1-hydroxy-allyl)-6-hydroxyl-2-*O*-phenoxythiocarbonyl-β-D-ribofuranosyl]-thymine (11). Compound **10** (6.7g, 13.6 mmol) was coevaporated thrice with anhydrous pyridine and dissolved in the same solvent (250 mL). The solution was cooled to −5 °C, and then phenyl chlorothionoformate was added dropwise (2.43 mL, 17.6 mmol), while temperature was maintained at ∼−5 °C during addition. After 3 h of stirring at room temperature, pyridine was recovered under reduced pressure. The residue was dissoloved in CH_2Cl_2 and washed with saturated solution of $NaHCO_3$ twice. The organic layer was separated, dried over $MgSO_4$, and concentrated. Crude product was chromatographed over silica gel (0−2 % methanol in CH_2Cl_2, v/v) to give **11** as white foam (8.1 g, 92%). ^{1}H NMR (600 MHz, $CDCl_3$): δ 9.18 (1H, s, N$\underline{H}$), 7.54 (1H, s, H6), 7.27−7.40 (13H, m, aromatic), 7.12 (2H, d, J = 7.80 Hz, aromatic), 6.43 (1H, d, $J_{H1',H2'}$ = 5.4 Hz, H1′), 5.96 (1H, m, H7′), 5.49 (1H, app t, J = 5.4 Hz, H2′), 5.39 (1H, dd, J = 1.80 Hz, 17.4 Hz, H8′), 5.26 (1H, dd, J = 1.80 Hz, 10.8Hz, H8′), 4,91(1H, d, J_{gem} = 11.4 Hz, C$\underline{H}_2$Bn), 4.72 (1H, m, H6′), 4.66 (1H, d, $J_{H3',H2'}$ = 5.4 Hz, H3′), 4.47−4.56 (3H, m, C$\underline{H}_2$Bn), 3.82 (1H, d, J_{gem} = 10.8 Hz, H5′), 3.71 (1H, d, J_{gem} = 10.8 Hz, H5″), 2.92 (1H, m, 6′-OH), 1.47 (3H, s, T-C$\underline{H}_3$). ^{13}C NMR (150 MHz): δ163.7 (C4), 152.9 (C$\underline{=}$S), 150.5, 150.4 (C2), 136.9 (Bn), 136.4 (Bn), 135.3 (C6), 134.4 (C7′) 129.6, 128.9, 128.6, 128.2, 127.6, 126.4, 120.8, (aromatic), 116.4 (C8′), 111.5 (C5), 87.4 (C4′), 85.8 (C1′), 78.6 (C2′), 78.1 (C3′), 75.1 (C$\underline{H}_2$Bn), 73.6 (C$\underline{H}_2$Bn), 71.7 (C6′), 69.3 (C5′), 12.0 (T-CH_3). MALDI-TOF *m*/*z*: $[M + Na]^+$ 653.1, calcd 653.2.

(1*R*,3*R*,4*R*,5*S*,6*S*,7*S*)-7-Benzyloxy-1-benzyloxmethyl-6-hydroxyl-5-methlyl-3-(thymin-1-yl)-2-oxa-bicyclo[2.2.1]heptane (12a) and (1*R*,3*R*,4*R*,5*R*,6*S*,7*S*)-7-Benzyloxy-1-benzyloxmethyl-6-hydroxyl-5-methyl-3-(thymin-1-yl)-2-oxa-bicyclo[2.2.1]heptane (12b). Compound **11** (4.2 g, 5.5 mmol) was dissolved in 200 mL of anhydrous toluene to which N_2 was purged for half an hour. The mixture was heated to reflux and Bn_3SnH (1.85 mL in 20 mL anhydrous toluene), AIBN (0.55 g in 20 mL anhydrous toluene) were added dropwise in 2 h. After 0.5 h, the reaction was found to be incomplete (TLC). Hence, a second portion of Bn_3SnH (0.9 mL in 10 mL toluene) and AIBN (0.25 g in 10 mL toluene) was added dropwise in 1 h, and reflux was continued for 1 h. Solvent was evaporated, and residue was applied to silica short column chromatography (EtOAc/cyclohexane, 2/8 to 6/4) to give 1.3 g of compound **12a** (49%), 0.32 g of **12b** (12%), and 0.7 g of recovered substrate. **12a**: ^{1}H NMR (600 MHz, $CDCl_3$): δ 8.87 (1H, broad, N$\underline{H}$), 7.72 (1H, s, H6), 7.34-7.23 (10H, m, aromatic), 5.75 (1H, s, H1′), 4.61-4.42 (4H, m, BnC$\underline{H}_2$), 4.15 (1H, t, $J_{6'H,6'OH}$ = 11.6 Hz, $J_{6'H,7'H}$ = 9.2 Hz, H6′), 4.05 (1H, s, 3′H), 3.91(1H, d, J_{gem} = 11.0 Hz, 5′H), 3.81 (1H, d, J_{gem} = 11.0 Hz, 5″H), 2.72 (1H, m, H7′), 2.66 (1H, d, $J_{2',H7'}$ = 4.5 Hz, 2′H), 2.25 (1H, d, $J_{6'H,6'OH}$ = 11.6 Hz, 6′OH), 1.50 (s, 3H, T-C$\underline{H}_3$), 1.15 (3H, d, $J_{7'\text{-}CH3,\ H7'}$ = 7.6 Hz, 7′C$\underline{H}_3$).^{13}C NMR (150 MHz, $CDCl_3$): δ 164.0 (C4), 149.9(C2), 137.6, 137.0, 136.0 (C6), 128.6, 128.5, 128.1, 127.9, 127.6, 109.6 (C5), 89.1 (C4′), 83.8 (C1′), 76.8 (C3′), 73.9 (BnC$\underline{H}_2$), 72.1 (BnC$\underline{H}_2$), 71.9 (C6′), 66.2 (C5′), 47.8 (C2′), 33.1 (C7′), 12.1 (T-C$\underline{H}_3$), 8.4 (7′C$\underline{H}_3$). MALDI-TOF *m*/*z*: $[M + Na]^+$ 501.221, calcd 501.200. **12b**: ^{1}H NMR (600 MHz, $CDCl_3$): δ 8.71 (1H, s, N$\underline{H}$), 7.75 (1H, s, H6), 7.22−7.34 (10H, m, aromatic), 5.50 (1H, s, H1′), 4.40−4.62 (4H, m, BnC$\underline{H}_2$), 4.04 (1H, s, 3′H), 4.00 (1H, dd, $J_{6'H,6'OH}$ = 11.0 Hz, $J_{6'H,7'H}$ = 3.7 Hz, 6′H), 3.93 (1H, d, J_{gem} = 11.0 Hz, 5′H), 3.83 (1H, d, J_{gem} = 11.0 Hz, 5″H), 2.55 (1H, s, 2′H), 2.23 (1H, d, $J_{6'H,6'OH}$ = 11.0 Hz, 6′OH), 1.77 (m, 1H, 7′H), 1.47 (3H, s, T-C$\underline{H}_3$), 1.31 (3H, d, $J_{7'CH3,7'H}$ = 7.3 Hz, 7′C$\underline{H}_3$).^{13}C NMR (150 MHz, $CDCl_3$): δ 163.8 (C4) 149.9 (C2), 137.5, 136.8, 135.9, 128.6, 128.5, 128.1, 128.0, 127.9, 127.5, 109.5 (C5), 88.9 (C4′), 88.6 (C1′), 81.0 (C6′), 79.0 (C3′), 73.9 (BnC$\underline{H}_2$), 72.4 (BnC$\underline{H}_2$), 65.8 (C5′), 45.3 (C2′), 42.1 (C7′), 18.1 (7′C$\underline{H}_3$), 12.0 (T-C$\underline{H}_3$). MALDI-TOF *m*/*z*: $[M + Na]^+$ 501.222, calcd 501.200.

(1*R*,3*R*,4*R*,5*S*,7*S*)-7-Benzyloxy-1-benzyloxmethyl-5-methyl-6-one-3-(thymin-1-yl)-2-oxa-bicyclo[2.2.1]heptane (13a). Compound **12a** (551 mg, 1.15 mmol) was dissolved in anhydrous CH_2Cl_2 (3 mL), and 15% Dess−Martin periodinane in CH_2Cl_2 (3.2 mL, 1.5 mmol) was added dropwise under nitrogen. After stirring at

room temperature for 2 h, the reaction mixture was diluted with CH_2Cl_2 and filtered through celite. The filtrate was washed with saturated $Na_2S_2O_3$ solution and $NaHCO_3$ successively and dried over $MgSO_4$. After evaporation of solvent under reduced pressure pure ketone **13a** was obtained quantitatively. ^{1}H NMR (500 MHz, $CDCl_3$): δ 8.72 (1H, broad, NH), 7.70 (1H, s, H6), 7.35-7.19 (10H, m, aromatic), 5.76 (1H, s, H1′), 4.64-4.49 (4H, m, BnCH_2), 4.26 (1H, s, H3′), 4.00 (1H, d, J_{gem} = 11.5 Hz, H5′), 3.85 (1H, d, J_{gem} = 11.5 Hz, H5″), 3.08 (1H, m, H2′), 2.86 (1H, m, H7′), 1.54 (3H, s, T-CH_3), 1.33 (3H, d, $J_{7',7'Me}$ = 7.5 Hz, 7′-Me). ^{13}C-NMR (125 MHz, $CDCl_3$): δ 206.6 (C=O), 163.8 (C4), 149.8 (C2), 137.3, 136.4, 135.7, 128.7, 128.6, 128.3, 128.2, 127.9, 127.6, 109.9 (C5), 86.3 (C4′), 84.0(C1′), 75.7 (C3′), 74.1, 72.3 (BnCH_2), 63.2 (C5′), 46.4 (C2′), 40.3 (C7′), 12.1 (T-Me), 9.5 (7′-Me). MALDI-TOF *m/z*: $[M + Na]^+$ 499.208, calcd 499.184.

(1*R*,3*R*,4*R*,5*S*,6*R*,7*S*)-7-Benzyloxy-1-benzyloxmethyl-6-hydroxyl-5-methyl-3-(thymin-1-yl)-2-oxa-bicyclo[2.2.1]heptane (14a). The ketone **13a** (548 mg, 1.15 mmol) was dissolved in 95% ethanol (15 mL), and $NaBH_4$ (47 mg, 1.24 mmol) was added in portions. The mixture was allowed to stir at room temperature for 2 h. Then solvent was removed, and the residue was extracted with CH_2Cl_2. The organic layer was washed with saturated $NaHCO_3$, dried over $MgSO_4$, and evaporated to give crude product, which was subjected to short column chromatography on silica gel (ethyl acetat in cyclohexane, 20−60% v/v) to give **14a** (297 mg, 54%) and 219 mg of **12a** (40%). ^{1}H NMR (500 MHz, $CDCl_3$): δ 8.75 (broad, H3), 7.72 (s, 1H, H6), 7.36-7.22 (10H, m, aromatic), 5.59 (1H, s, H1′), 4.65-4.44 (4H, m, BnCH_2), 4.17 (s, 1H, H3′), 4.04 (1H, d, J_{gem} = 11.3 Hz, H5′), 3.96 (1H, d, J_{gem} = 11.3 Hz, H5″), 3.32 (1H, dt, $^3J_{6'H,6'OH}$ = 12.2 Hz, $^WJ_{6'H,3'H}$ = 1.8 Hz, $^3J_{6'H,7'H}$ = 3.4 Hz, H6′), 2.82 (1H, d, $^3J_{2'H,7'H}$ = 3.4 Hz, H2′), 2.46 (1H, d, $^3J_{6'H,6'OH}$ = 12.2 Hz, 6′OH), 2.31 (1H, m, H7′), 1.52 (3H, s, T-CH_3), 1.36 (3H, d, $J_{7',7'Me}$ = 7.3 Hz, 7′-Me). ^{13}C NMR (125 MHz, $CDCl_3$): δ 163.9 (C4), 149.9 (C2), 137.6, 136.3, 136.1, 128.7, 128.6, 128.5, 128.1, 128.0, 127.9, 109.5 (C5), 86.9 (C4′), 83.7(C1′), 81.0 (C6′), 79.5 (C3′), 73.9, 72.5 (BnCH_2), 65.7 (C5′), 47.2 (C2′), 42.2 (C7′), 13.4 (7′-Me), 12.1 (T-Me). MALDI-TOF *m/z*: $[M + H]^+$ 479.217, calcd 479.218.

(1*R*,3*R*,4*R*,5*S*,6*S*,7*S*)-7-Benzyloxy-1-benzyloxymethyl-5-methyl-6-(4-methylbenzoate)-3-(thymin-1-yl)-2-oxa-bicyclo[2.2.1]heptane (15a). The compound **12a** (291 mg, 0.6 mmol) was coevaporated with anhydrous pyridine twice and dissolved in anhydrous CH_2Cl_2 (5 mL), to which was added anhydrous pyridine 0.2 mL. The mixture was cooled to −5 °C, and 4-methyl benzoyl chloride (0.1 mL, 0.72 mmol) was added. The mixture was allowed to stir at room temperature for 2 h. Pyridine was recovered under reduced pressure, and the residue was dissoloved in CH_2Cl_2. The obtained solution was washed with a saturated solution of $NaHCO_3$, dried with $MgSO_4$, and concentrated under reduced pressure to give crude product, which was subjected to short column chromatography on silica gel (20−30 % ethyl acetate in cyclohexane, v/v) to give **15a** (278 mg, 78%). ^{1}H NMR (500 MHz, $CDCl_3$): δ 8.67 (s, 1H, NH), 7.99 (2H, d, J = 8.5 Hz, aromatic), 7.84 (1H, s, H6), 7.38-7.27 (12H, m, aromatic), 5.93 (1H, s, H1′), 5.50 (1H, d, J = 9.5 Hz, H6′), 4.63-4.51 (4H, m, CH_2Bn), 4.17 (1H, s, H3′), 3.78 (2H, dd, J_{gem} = 11.5 Hz, H5′, H5″), 3.04 (1H, m, H7′), 2.76 (1H, d, J = 3.5 Hz, H2′), 2.45 (3H, s, Tol-CH_3), 1.51 (3H, s, T-CH_3), 1.08 (3H, d, J = 8.0 Hz, 7′-CH_3). ^{13}C NMR (125 MHz, $CDCl_3$): δ 166.5 (C=O), 163.9 (C4), 149.8 (C2), 144.2, 137.6, 136.9, 136.1, 129.8, 129.2, 128.6, 128.5, 128.7, 128.0, 127.8, 127.6, 126.9, 109.5 (C5), 88.7 (C4′), 83.8 (C1′), 77.5 (C3′), 74.0(C6′), 73.9 (CH_2Bn), 72.3 (CH_2Bn), 66.3 (C5′), 48.1 (C2′), 32.8 (C7′), 21.7(Tol-Me), 11.9 (T-Me), 8.9 (7′-Me). MALDI-TOF *m/z*: $[M + H]^+$ 597.2, calcd 597.2.

(1*R*,3*R*,4*R*,5*S*,6*S*,7*S*)-1-(4,4′-Dimethoxytrityloxymethyl)-7-hyroxyl -5-methyl-6-(4-methylbenzoate)-3-(thymin-1-yl)-2-oxa-bicyclo[2.2.1]heptane (16a). To a solution of compound **15a** (285 mg, 0.48 mmol) in anhydrous methanol (5 mL) was added 20% $Pd(OH)_2$/C (0.72 g) and ammonium formate (1.8 g, 28.7 mmol), and the mixture was refluxed for 2 h. The suspension was filtered over celite, and the organic phase was evaporated to give crude **15a′**, which was co-evaporated twice with anhydrous pyridine and dissolved in the same solvent (5 mL). 4,4′-Dimethoxytrityl chloride (178 mg, 0.53 mmol) was added, and the mixture was stirred for 2 h at room temperature. Then solvent was removed, and the residue was diluted with CH_2Cl_2, washed with saturatured $NaHCO_3$, and dried over $MgSO_4$. After evaporation of solvent, the residue was subjected to column chromatography on silica gel (methanol in CH_2Cl_2 containing 1% pyridine, 0.5−1.5%, v/v) to obtain **16a** (240 mg, 70 %). ^{1}H NMR (500 MHz, $CDCl_3$): δ 7.93 (2H, d, J = 8.5 Hz, aromatic), 7.78 (1H, s, H6), 7.47−6.82 (15H, m, aromatic), 5.89 (1H, s, H1′), 5.41 (1H, d, J = 9.5 Hz, H6′), 4.31 (1H, d, J = 1.5 Hz, H3′), 3.78 (6H, s, MeO), 3.69 (1H, dd, J_{gem} = 11.5 Hz, H5′), 3.52 (1H, dd, J_{gem} = 11.5 Hz, H5″), 3.09 (1H, m, H7′), 2.64 (1H, m, H2′), 2.44 (3H, s, tol-CH_3), 1.45 (3H, s, T-CH_3), 1.15 (3H, d, J = 7.5 Hz, 7′-CH_3). ^{13}C NMR (125 MHz, $CDCl_3$): δ 166.2, 163.9, 158.6, 149.6 (C2), 144.2, 139.8, 135.4, 135.3, 135.2, 129.9, 129.7, 129.1, 128.0, 127.9, 127.1, 113.3, 109.6 (C5), 88.6, 87.0, 83.7, 73.9, 72.5, 59.6, 55.1, 46.5, 32.4, 21.5, 12.2, 8.5 (7′-Me). MALDI-TOF *m/z*: $[M + K]^+$ 757.3, calcd 757.3.

(1*R*,3*R*,4*R*,5*S*,6*S*,7*S*)-7-Benzyloxy-1-benzyloxmethyl-6-hydroxyl-5,6-dimethyl-3-(thymin-1-yl)-2-oxa-bicyclo[2.2.1]heptane (18a) and (1*R*,3*R*,4*R*,5*S*,6*R*,7*S*)-7-Benzyloxy-1-benzyloxmethyl-6-hydroxyl-5,6-dimethyl-3-(thymin-1-yl)-2-oxa-bicyclo[2.2.1]heptane (18b). MeMgI (3 M in ether, 3.48 mL, 10.45 mmol) was added dropwise to the solution of compound **13a** (0.87 g, 1.82 mmol) in anhydrous THF (30 mL) at 0 °C under nitrogen. After stirring at room temperature for 3 h, the reaction was quenched with saturated NH_4Cl solution and extracted with CH_2Cl_2. The organic layer was separated, dried over $MgSO_4$, and concentrated. Residue was chromatographed on silica gel (methanol in CH_2Cl_2, 0−2%, v/v) to give **18a** (391 mg, 43%) and **18b** (157 mg, 18%). **18a**: ^{1}H NMR (500 MHz, $CDCl_3$): δ 8.62 (1H, brs, NH), 7.71 (1H, s, H6), 7.36-7.25 (10H, m, aromatic), 5.72 (1H, s, H1′), 4.63-4.45 (4H, m, CH_2Bn), 4.06 (1H, s, H3′), 3.89 (2H, s, H5′, H5″), 2.81 (1H, s, 6′-OH), 2.62(1H, d, $J_{H2',H7'}$ = 3.7 Hz, H2′), 2.41(1H, m, H7′), 1.51 (3H, s, T-CH_3), 1.33 (3H, s, 6′-Me), 1.13 (3H, d, J = 7.6 Hz, 7′-CH_3). ^{13}C NMR (125 MHz, $CDCl_3$): δ 163.8 (C4), 149.7 (C2), 137.4, 136.9, 136.0 (C6), 128.6-127.6 (aromatic), 109.5 (C5), 89.8 (C4′), 82.9 (C1′), 77.2, 76.7 (C3′, C6′), 74.0, 72.2 (CH_2Bn), 64.6 (C5′), 48.2 (C2′), 40.1 (C7′), 23.6 (6′-CH_3), 12.0 (T-CH_3), 8.3 (7′-CH_3). MALDI-TOF *m/z*: $[M + Na]^+$ found 515.231, calcd 515.215. **18b**: ^{1}H NMR (500 MHz, $CDCl_3$): δ 8.66 (1H, brs, NH), 7.69 (1H, s, H6), 7.34-7.23 (10H, m, aromatic), 5.53 (1H, s, H1′), 4.64-4.48 (4H, m, CH_2Bn), 4.16 (1H, s, H3′), 4.06 (1H, d, J_{gem} = 11.0 Hz, H5′), 3.87 (1H, d, J_{gem} = 11.0 Hz, H5″), 3.35 (1H, s, 6′-OH), 2.71(1H, d, $J_{H2',H7'}$ = 4.3 Hz, H2′), 2.46(1H, m, H7′), 1.51 (3H, s, T-CH_3), 1.20 (3H, d, $J_{H7',7'Me}$ = 7.6 Hz, 7′-CH_3), 1.14 (3H, s, 6′-Me). ^{13}C-NMR (125 MHz, $CDCl_3$): δ 164.3 (C4), 150.2 (C2), 138.1, 136.6, 136.4 (C6), 129.1, 128.9, 128.8, 128.4, 128.2, 109.8 (C5), 88.3 (C4′), 83.3 (C1′), 79.3 (C6′), 78.8 (C3′), 74.4, 73.1 (CH_2Bn), 65.2 (C5′), 48.5 (C2′), 45.2 (C7′), 16.8 (6′-CH_3), 12.0 (T-CH_3), 10.6 (7′-CH_3). MALDI-TOF *m/z*: $[M + Na]^+$ 515.249, calcd 515.215.

(1*R*,3*R*,4*R*,5*S*,6*S*,7*S*)-7-Benzyloxy-1-benzyloxmethyl-5,6-dimethyl-6-methoxalyloxy-3-(thymin-1-yl)-2-oxa-bicyclo[2.2.1]heptane (21). Methyl oxalyl chloride (0.1 mL, 1.08 mmol) was added to the solution of compound **18a** (351 mg, 0.72 mmol) in anhydrous MeCN (5 mL) containing DMAP (175 mg, 1.44 mmol) under nitrogen. After stirring at room temperature for 2 h, another portion of methyl oxalyl chloride (0.1 mL, 1.08 mmol) and DMAP (175 mg, 1.44 mmol) was added, and the mixture was stirred for further 2 h. Solvent was removed, and the residue obtained was dissolved in CH_2Cl_2, which was washed with saturated $NaHCO_3$ solution, dried over $MgSO_4$, and evaporated. The residue was purified by column chromatography on silica gel (20−35 % ethyl acetate in cyclohexane, v/v) to obtain **21** (393 mg, 94%) as white solid. ^{1}H NMR (500 MHz, $CDCl_3$): δ 8.44 (1H, brs, H3), 7.64 (1H, s, H6),

7.34-7.26 (10H, m, aromatic), 5.77 (1H, s, H1′), 4.67 (4H, m, C$\underline{H}_2$Bn), 4.39 (1H, d, J_{gem} = 11.5 Hz, H5′), 4.24 (1H, s, H3′), 4.03 (1H, d, J_{gem} = 11.5 Hz, H5″), 3.90 (3H, s, CH_3- methyl oxalyl), 2.64 (1H, m, H7′), 2.52 (1H, s, H2′), 1.72 (3H, s, 6′-C$\underline{H}_3$), 1.54 (3H, s, T-C$\underline{H}_3$), 1.33 (3H, d, $J_{7'\text{-Me},7'}$ = 7.0 Hz, 7′-C$\underline{H}_3$). ^{13}C NMR (125 MHz, $CDCl_3$): δ 163.7 (C4), 158.3, 156.5 (C═O methyl oxalyl), 149.7 (C2), 137.8, 136.9, 135.9 (C6), 128.5-127.7 (aromatic), 109.6 (C5), 89.8, 89.7, 83.1 (C1′), 78.7 (C3′), 73.7, 72.5 (C$\underline{H}_2$Bn), 66.4 (C5′), 53.6 (C$\underline{H}_3$- methyl oxalyl), 48.1 (C2′), 42.9 (C7′), 20.6 (6′C$\underline{H}_3$), 12.1 (T-C$\underline{H}_3$), 8.9 (7′-C$\underline{H}_3$). MALDI-TOF *m*/*z*: $[M + H]^+$ 579.2, calcd 579.2.

(1*R*,3*R*,4*R*,5*S*,6*S*,7*S*)-7-Benzyloxy-1-benzyloxmethyl-5,6-dimethyl-3-(thymin-1-yl)-2-oxa-bicyclo[2.2.1] heptane (22a) and (1*R*,3*R*,4*R*,5*S*,6*R*,7*S*)-7-Benzyloxy-1-benzyloxmethyl-5,6-dimethyl-3-(thymin-1-yl)-2-oxa-bicyclo[2.2.1]heptane (22b). Compound **21** (210 mg, 0.36 mmol) was dissolved in anhydrous toluene (10 mL) and purged with anhydrous nitrogen for 30 min. AIBN (30 mg, 0.18 mmol) and Bu_3SnH (0.29 mL, 1.08 mmol) were added to the mixture, which was refluxed for 0.5 h. The reaction mixture was cooled to room temperature and evaporated. The residue was chromatographed over silica gel (20−35% ethyl acetate in cyclohexane, v/v) to obtain **22a** and **22b** as a mixture (57mg, 33.3%, **22a**/**22b** = 4/3). **22a**: ^{1}H NMR (500MHz, $CDCl_3$): δ 8.19 (1H, brs, N$\underline{H}$), 7.81(1H, s, H6), 7.38-7.27 (10H, m, aromatic), 5.71 (1H, s, H1′), 4.65-4.43 (4H, m, C$\underline{H}_2$Bn), 4.06 (1H, s, H3′), 3.79 (1H, d, J_{gem} = 11.0 Hz, H5′), 3.70 (1H, d, J_{gem} = 11.0 Hz, H5″), 2.72 (1H, m, H7′), 2.57(1H, d, $J_{H2',H7'}$ = 4.0 Hz, H2′), 2.30 (1H, m, H6′), 1.54 (3H, s, T-CH_3), 1.14 (3H, d, $J_{7'\text{-Me},7'}$ = 7.6 Hz, 7′-C$\underline{H}_3$), 0.92 (3H, d, $J_{H6',\ 6'\text{-}CH3}$ = 7.3 Hz, 6′-C$\underline{H}_3$). ^{13}C NMR (125 MHz, $CDCl_3$): δ 163.8 (C4), 149.73 (C2), 137.9, 137.6, 136.5 (C6), 128.5-127.5 (aromatic), 109.1 (C5), 89.8 (C4′), 83.7 (C1′), 77.6 (C3′), 73.8, 71.9 (C$\underline{H}_2$Bn), 67.2 (C5′), 48.4 (C2′), 35.4 (C6′), 31.4 (C7′), 12.2 (T-C$\underline{H}_3$), 10.1 (7′-C$\underline{H}_3$), 8.0 (6′-C$\underline{H}_3$). **22b**: ^{1}H NMR (500 MHz, $CDCl_3$): δ 8.19 (1H, brs, N$\underline{H}$), 7.72 (1H, s, H6), 7.38-7-27 (10H, m, aromatic), 5.72 (1H, s, H1′), 4.65-4.43 (4H, m, C$\underline{H}_2$Bn), 4.03 (1H, s, H3′), 3.85 (2H, s, H5′, H5″), 2.64 (1H, d, $J_{H2',H7'}$ = 4.0 Hz, H2′), 2.21 (1H, m, H7′), 1.58 (3H, s, T-C$\underline{H}_3$), 1.55 (1H, m, H6′), 1.28 (3H, d, $J_{7'\text{-Me},7'}$ = 7.3 Hz, 7′-C$\underline{H}_3$), 1.07 (3H, d, $J_{6',6'\text{-}CH3}$ = 7.3 Hz, 6′-C$\underline{H}_3$). ^{13}C NMR (125 MHz, $CDCl_3$) : δ 163.8 (C4), 149.70 (C2), 137.8, 137.5, 136.4 (C6), 128.5-127.5 (aromatic), 109.1 (C5), 89.1 (C4′), 83.8 (C1′), 79.6 (C3′), 73.8, 71.9 (C$\underline{H}_2$Bn), 66.8 (C5′), 47.2 (C6′), 38.2 (C7′), 15.3 (6′-C$\underline{H}_3$), 13.9 (7′-C$\underline{H}_3$), 12.2 (T-C$\underline{H}$3). MALDI-TOF *m*/*z*: $[M + Na]^+$ 499.236, calcd 499.221.

General Procedure for Phosphoramidite Synthesis. The substrate (1 equiv) was dissolved in anhydrous THF to which was added DIPEA (5 equiv) followed by 2-cyanoethyl-*N*,*N*-diisopropyl phosphoramidochloridite (2 equiv) in an ice bath. The reaction mixture was allowed to warm to room temperature and stirred at this temperature for 2−4 h. After being quenched with methanol, the reaction mixture was extracted with ethyl acetate and washed with saturated $NaHCO_3$ solution, dried over $MgSO_4$, and concentrated. The residue was subjected to short column chromatography on silica gel to give pure phosphoramidite, which was first precipitated in *n*-hexane and then dried over P_2O_5 on vacuum for 3 days before it was used for DNA synthesis.

Oligonucleotide Synthesis and Purification. All AONs were synthesized using an automated DNA/RNA synthesizer based on phosphoramidite chemistry. For native A, G, and C building blocks, fast deprotecting phosphoramidites (Ac for C, *i*Pr-Pac for G, Pac for A) were used. Standard DNA synthesis reagents and cycles were used except that 0.25 M 5-ethylthio-1*H*-tetrazole was used as the activator and Tac_2O as cap A. For incorporating modified nucleotides, extended coupling time (10 min comparing to 25 s for native nucleotides) was used. For AONs **6**−**13** and **37**−**40** the deprotections were carried out in 33% aqueous NH_3 for 16 h at 55 °C. For AONs **14**−**21** and **41**−**44** the deprotections were carried out in 33% aqueous NH_3 for 72 h at 55 °C. Other oligoes were deprotected at room temperature by treatment with 33% aqueous NH_3 for 12h. After deprotection, all crude oligoes were purified by denaturing PAGE (20% polyacrylamide with 7 M urea), extracted with 0.3 M NaOAc, and desalted with a C-18 reverse phase cartridge to give AONs in >99% purity, and correct masses have been obtained by MALDI-TOF mass spectroscopy for each of them (Table 1).

RNA was also synthesized by a solid-supported phosphoramidite approach based on the 2′-O-TEM strategy.[51,52]

UV Melting Experiments. Determination of the T_m of the AON/RNA hybrids or AON/DNA duplex was carried out in the following buffer: 60 mM Tris-HCl (pH 7.5), 60 mM KCl, 0.8 mM $MgCl_2$. Absorbance was monitored at 260 nm in the temperature range from 20 to 70 °C using an UV spectrophotometer equipped with a Peltier temperature programmer with the heating rate of 1 °C/min. Prior to measurements, the samples (1 μM AON and 1 μM complementary DNA or RNA mixture) were preannealed by heating to 80 °C for 5 min followed by slow cooling to 21 °C and 30 min equilibration at this temperature. The value of T_m is the average of two or three independent measurements. If error of the first two measurements was greater than ±0.3 °C, the third measurement was carried out to check if the error is indeed within ±0.3 °C; otherwise it was repeated again.

^{32}P Labeling of Oligonucleotides. The oligoribonucleotides and oligodeoxyribonucleotides were 5′-end labeled with ^{32}P using T4 polynucleotide kinase, [γ-^{32}P]ATP, and the standard protocol. Labeled AONs and the target RNA were purified by QIAquick Nucleotide Removal Kit, and specific activities were measured using a Beckman LS 3801 counter.

SVPDE Degradation Studies. Stability of the AONs toward 3′-exonucleases was tested using phosphodiesterase I from *Crotalus adamanteus* (obtained from USB corporation, Cleveland, OH). All reactions were performed at 3 μM DNA concentration (5′-end ^{32}P labeled with specific activity 80 000 cpm) in 100 mM Tris-HCl (pH 8.0) and 15 mM $MgCl_2$ at 21 °C. An exonuclease concentration of 6.7 or 2.2 ng/μL was used for digestion of oligonucleotides. Total reaction volume was 30 μL. Aliquots (3 μL) were taken at proper time points and quenched by the addition of stop solution (4 μL) [containing 0.05 M EDTA, 0.05% (w/v) bromophenol blue, and 0.05% (w/v) xylene cyanole in 80% formamide]. Reaction progress was monitored by 20% denaturing (7 M urea) PAGE and autoradiography.

The total percentage of integrated AONs (13−15mer) were plotted against time points to give the digestion curves, and the pseudo-first-order reaction rates could be obtained by fitting the curves to single-exponential decay functions.

Stability Studies in Human Blood Serum. AONs at 2 μM concentration (5′-end ^{32}P-labeled with specific activity 80 000 cpm) were incubated in 10 μL of human blood serum (male AB, obtained from Sigma-Aldrich) at 21 °C (total reaction volume was 36 μL). Aliquots (3 μL) were taken at the proper time points, quenched with 4 μL of stop solution [containing 0.05 M EDTA, 0.05% (w/v) bromophenol blue, and 0.05% (w/v) xylene cyanole in 80% formamide], resolved in 20% polyacrylamide denaturing (7 M urea) gel electrophoresis, and visualized by autoradiography.

RNase H Digestion Assay. Target 0.1 μM RNA (specific activity 80 000 cpm) and AON (2 μM) were incubated in a buffer containing 20 mM Tris-HCl (pH 7.5), 20 mM KCl, 10 mM $MgCl_2$, 0.1 mM EDTA, and 0.1 mM DTT at 21 °C in the presence of 0.08 U of *E. coli* RNase H (obtained from USB corporation, Cleveland, OH). Prior to the addition of the enzyme, reaction components were preannealed in the reaction buffer by heating at 80 °C for 5 min followed by slow cooling to 21°C and 30 min equilibration at this temperature. Total reaction volume was 30 μL. Aliquots of 3 μL were removed after 5, 10, 15, 30, and 60 min, and the reactions were terminated by mixing with stop solution [containing 0.05 M EDTA, 0.05% (w/v) bromophenol blue, and 0.05% (w/v) xylene

(51) Zhou, C.; Honcharenko, D.; Chattopadhyaya, J. *Org. Biomol. Chem.* **2007**, *5*, 333–343.
(52) Zhou, C.; Pathmasiri, W.; Honcharenko, D.; Chatterjee, S.; Barman, J.; Chattopadhyaya, J. *Can. J. Chem* **2007**, *85*, 293–301.

cyanole in 80% formamide]. The samples were subjected to 20% 7 M urea PAGE and visualized by autoradiography. Pseudo-first-order reaction rates could be obtained by fitting the digestion curves to single-exponential decay functions.

Theoretical Calculations. Methyl- and hydroxyl-substituted carba-LNA nucleosides were investigated in silico using ab initio technique. The geometry optimizations of the modified nucleosides were carried out using the GAUSSIAN 98 program package[53] at the Hartree-Fock level using 6-31G**. Relevant vicinal proton $^3J_{H,H}$ coupling constants have been back-calculated from the corresponding theoretical torsions employing the Haasnoot−de Leeuw−Altona generalized Karplus equation[43,44] taking into account β substituent correction in the form

$$^3J = P_1 \cos^2(\varphi) + P_2 \cos(\varphi) + P_3 + \sum \Delta\chi_i^{\text{group}}\left(P_4 + P_5 \cos^2\left(\xi_i\varphi + P_6|\Delta\chi_i^{\text{group}}|\right)\right) \quad (1)$$

where $P_1 = 13.70$, $P_2 = -0.73$, $P_3 = 0.00$, $P_4 = 0.56$, $P_5 = -2.47$, $P_6 = 16.90$, $P_7 = 0.14$ (parameters from ref 43), and $\Delta\chi_i^{\text{group}} = \Delta\chi_i^{\alpha\text{-substituent}} - P_7\,\Sigma\Delta\chi_i^{\beta\text{-substituent}}$ where $\Delta\chi_i$ are taken as Huggins electronegativities.[54]

Acknowledgment. Generous financial support from the Swedish Natural Science Research Council (Vetenskapsrådet), the Swedish Foundation for Strategic Research (Stiftelsen för Strategisk Forskning), and the EU-FP6 funded RIGHT project (Project no. LSHB-CT-2004-005276) is gratefully acknowledged. Individual authors' contributions on this work can be found in SI Part IV.

Supporting Information Available: ^{1}H, ^{13}C, ^{31}P, DEPT, COSY, HMQC, and HMBC of carba-LNA derivatives (SI part I) and carba-ENA derivatives (SI part II); 1D NOE and 2D NOESY spectra, experimental and calculated coupling constants of key intermediates **12**, **14**, **18**, **22**, **30**, **31**, **33**, **35**, and **36**; autoradiograms of 20% denaturing PAGE of digestion of AONs in SVPDE. Autoradiograms of 20% denaturing PAGE as well as degradation curves, showing the cleavage kinetics of target RNA in AON/RNA hybrides by *E. coli* RNase H1(SI Part III); a brief description of Schemes 4 and 5; discussion about configuration determination on chiral center by NOE experiment, how the position and stereochemical orientation of various substitutents on the carbocyclic moiety affects the T_m's; RNA/DNA duplex model to show the location of subsitituents in the carbocylic moeity in the duplex (SI Part IV). This material is available free of charge via the Internet at http://pubs.acs.org.

JO8016742

(53) Frisch, M. J., et al. *Gaussian 98 (Revision A.6)*; Gaussian, Inc: Pittsburgh, PA, 1998.

(54) Huggins, M. L. *J. Am. Chem. Soc.* **1953**, *75*, 4123–4126.